UC Irvine
UC Irvine Previously Published Works

Title

Unique Type I Interferon, Expansion/Survival Cytokines, and JAK/STAT Gene Signatures of Multifunctional Herpes Simplex Virus-Specific Effector Memory CD8+ TEM Cells Are Associated with Asymptomatic Herpes in Humans.

Permalink

https://escholarship.org/uc/item/3pv8w2md

Journal

Journal of Virology, 93(4)

ISSN

0022-538X

Authors

Vahed, Hawa
Agrawal, Anshu
Srivastava, Ruchi
et al.

Publication Date

2019-02-15

DOI

10.1128/jvi.01882-18

Peer reviewed

AMERICAN SOCIETY FOR MICROBIOLOGY | Journal of Virology®

Unique Type I Interferon, Expansion/Survival Cytokines, and JAK/STAT Gene Signatures of Multifunctional Herpes Simplex Virus-Specific Effector Memory CD8+ T$_{EM}$ Cells Are Associated with Asymptomatic Herpes in Humans

Hawa Vahed,[a] Anshu Agrawal,[b] Ruchi Srivastava,[a] Swayam Prakash,[a] Pierre-Gregoire A. Coulon,[a] Soumyabrata Roy,[a] Lbachir BenMohamed[a,c,d]

[a]Laboratory of Cellular and Molecular Immunology, Gavin Herbert Eye Institute, University of California Irvine, School of Medicine, Irvine, California, USA
[b]Division of Basic and Clinical Immunology, Department of Medicine, University of California Irvine, School of Medicine, Irvine, California, USA
[c]Department of Molecular Biology and Biochemistry, University of California Irvine, School of Medicine, Irvine, California, USA
[d]Institute for Immunology, University of California Irvine, School of Medicine, Irvine, California, USA

ABSTRACT A large proportion of the world population harbors herpes simplex virus 1 (HSV-1), a major cause of infectious corneal blindness. HSV-specific CD8+ T cells protect from herpesvirus infection and disease. However, the genomic, phenotypic, and functional characteristics of CD8+ T cells associated with the protection seen in asymptomatic (ASYMP) individuals, who, despite being infected, never experienced any recurrent herpetic disease, remains to be fully elucidated. In this investigation, we compared the phenotype, function, and level of expression of a comprehensive panel of 579 immune genes of memory CD8+ T cells, sharing the same HSV-1 epitope specificities, and freshly isolated peripheral blood from well-characterized cohorts of protected ASYMP and nonprotected symptomatic (SYMP) individuals, with a history of numerous episodes of recurrent herpetic disease, using the high-throughput digital NanoString nCounter system and flow cytometry. Interestingly, our results demonstrated that memory CD8+ T cells from ASYMP individuals expressed a unique set of genes involved in expansion and survival, type I interferon (IFN-I), and JAK/STAT pathways. Frequent multifunctional HSV-specific effector memory CD62L^{low} CD44^{high} CD8+ T$_{EM}$ cells were detected in ASYMP individuals compared to more of monofunctional central memory CD62L^{high} CD44^{high} CD8+ T$_{CM}$ cells in SYMP individuals. Shedding light on the genotype, phenotype, and function of antiviral CD8+ T cells from "naturally protected" ASYMP individuals will help design future T-cell-based ocular herpes immunotherapeutic vaccines.

IMPORTANCE A staggering number of the world population harbors herpes simplex virus 1 (HSV-1) potentially leading to blinding recurrent herpetic disease. While the majority are asymptomatic (ASYMP) individuals who never experienced any recurrent herpetic disease, symptomatic (SYMP) individuals have a history of numerous episodes of recurrent ocular herpetic disease. This study elucidates the phenotype, the effector function, and the gene signatures of memory CD8+ T-cell populations associated with protection seen in ASYMP individuals. Frequent multifunctional HSV-specific effector memory CD8+ T$_{EM}$ cells were detected in ASYMP individuals. In contrast, nonprotected SYMP individuals had more central memory CD8+ T$_{CM}$ cells. The memory CD8+ T$_{EM}$ cells from ASYMP individuals expressed unique gene signatures characterized by higher levels of type I interferon (IFN), expansion and expansion/survival cytokines, and JAK/STAT pathways. Future studies on the genotype, phenotype, and function of antiviral CD8+ T cells from "naturally protected" ASYMP individuals will help in the potential design of T-cell-based ocular herpes vaccines.

A staggering number of individuals—3.72 billion worldwide—are currently infected with herpes simplex virus 1 (HSV-1) (1–5). The vast majority of these HSV-seropositive individuals are asymptomatic (ASYMP). They do not experience any recurrent ocular herpetic disease even though they constantly shed viral particles in tears (1–3, 6, 7). In contrast, some HSV-seropositive individuals are symptomatic (SYMP) and experience sporadic recurrent herpetic diseases which require antiviral drug therapy, such as acyclovir and derivatives (8, 9). If left untreated, corneal reinfection with HSV-1 can cause potentially blinding recurrent herpetic stromal keratitis (rHSK), lesions of the cornea that are mediated by immunopathological T cells (10–12). The nature of the mechanism(s) by which T cells lead to immunopathological herpetic disease in SYMP individuals and to immune protection in ASYMP individuals should inform the design of a future herpes immunotherapy.

Following a primary HSV-1 infection (13), the vast majority (up to 95%) of antiviral effector CD8+ T cells die, leaving behind only about 5% of CD8+ T cells destined to differentiate into a heterogeneous pool of memory CD8+ T cells (14–18). HSV-specific memory CD8+ T cells survive long-term in the absence of viral antigens (over 2 years in mice and over 50 years in humans) (2, 19, 20). Memory CD8+ T cells mediate recall responses that result in halting attempts of virus reactivation from latently infected tissues, and their maintenance is crucial in accelerating viral clearance. While memory CD8+ T cells are critical for long-term herpes immunity, a vaccine capable of generating robust T-cell memory remains a challenge, due, in part, to an incomplete understanding of the characteristics CD8+ T-cell subsets that are associated with herpes protection. Thus, identifying the key genotypes, phenotypes, and functions of various HSV-specific memory CD8+ T-cell subsets associated with protection observed in human ASYMP individuals is critical in the rational design of future herpes therapeutic vaccines.

In the present study, we used the high-throughput digital NanoString nCounter system and flow cytometry to interrogate the transcriptomes of individual CD8+ T-cell subsets and compare the genotypes, phenotypes, and functions of HSV-specific memory CD8+ T cells that shared the same epitope specificity but were freshly sorted from the peripheral blood of well-characterized cohorts of ASYMP and SYMP individuals, with a history of numerous episodes of recurrent herpetic disease. Our results indicate that regardless of the antigen specificity, circulating HSV-specific memory CD8+ T cells from ASYMP individuals (i) were predominately of the polyfunctional effector memory phenotype (i.e., CD62L^{low} CD44^{high} CD8+ T$_{EM}$ cells) and (ii) expressed unique gene signatures consistent with the active Janus kinase/signal transducer and activator of transcription (JAK/STAT) pathway, type I interferon (IFN), and interleukins involved in T-cell survival and expansion (e.g., *JAK2*, *STAT5B*, *SOCS1*, *SOCS3*, *IL-2*, *IL-4*, *IL-6*, *IL-6ST*, *IL-6R*, and *IL-7*). In contrast, HSV-specific CD8+ T$_{CM}$ cells derived from SYMP individuals (i) were predominately monofunctional central memory CD62L^{high} CD44^{high} CD8+ T$_{CM}$ cells and (ii) expressed low levels of JAK/STAT, IFN-I, and survival and expansion cytokine genes. These findings have profound implications in the development of T-cell-based immunotherapeutic strategies to treat herpes infection and disease.

RESULTS

Upregulation of multi-immune genes in HSV-specific CD8+ T cells from asymptomatic individuals compared to symptomatic individuals. The characteristics of the symptomatic (SYMP) and asymptomatic (ASYMP) study populations used in the present study, with respect to gender, age, HLA-A*02:01 frequency distribution, HSV-1/HSV-2 seropositivity, and status of ocular herpetic disease are presented in Table 1 and detailed in Materials and Methods. Since HSV-1 is the main cause of ocular herpes, only individuals who were HSV-1 seropositive and HSV-2 seronegative were enrolled in this study. The HSV-1-seropositive individuals were divided into two groups: (i) 10 HLA-A*02:01-positive ASYMP individuals who, despite being infected, never had any

TABLE 1 Cohorts of HLA-A*02:01-positive, HSV-seropositive symptomatic and asymptomatic individuals enrolled in the NanoString study

Subject characteristic	Value (n = 50)
Sex [no. (%)]	
Female	26 (52)
Male	24 (48)
Race [no. (%)]	
Caucasian	21 (42)
Non-Caucasian	29 (58)
Age [median (range), yr]	23 (22–66)
HSV status [no. (%)]	
HSV-1 seropositive	40 (80)
HSV-2 seropositive	00 (0)
HSV-1 and -2 seropositive	00 (0)
HSV seronegative	10 (20)
HLA status [no. (%)]	
HLA-A*02:01 positive	50 (100)
HLA-A*02:01 negative	00 (0)
Herpes disease status [no. (%)]	
ASYMP	20 (40)
SYMP	20 (40)

clinically detectable herpes disease and (ii) 10 HLA-A*02:01-positive SYMP individuals with a history of numerous episodes of clinically documented recurrent ocular herpes diseases, such as herpetic lid lesions, herpetic conjunctivitis, dendritic or geographic keratitis, stromal keratitis, and iritis consistent with rHSK, with one or more episodes per year for the past 5 years. Four patients had over 4 severe recurrent episodes during the last 10 years that necessitated corneal transplantations. Only SYMP patients who were not on acyclovir or other antiviral or anti-inflammatory drug treatments at the time of blood sample collections were enrolled. Ten age- and sex-matched HLA-A*0201-positive and HSV-1- and HSV-2-seronegative healthy (NEG) subjects were enrolled as controls.

We compared the immune gene signatures associated with HSV-specific CD8+ T cells from SYMP and ASYMP individuals that shared the same epitope specificity, using NanoString digital barcoding technology. We evaluated the level of expression of a comprehensive, customized panel of 579 immune genes, selected from published multigene immunology signatures. These immune genes are associated with various pathways (Table 2).

TABLE 2 Comprehensive panel of 579 immune genes used in NanoString

Immune gene distribution in panel	No. of genes in panel
Chemokine/cytokine	133
Cell function	112
Regulation	109
Signal transduction	85
Transcription factor	27
Adhesion molecules	26
Cell differentiation	25
Apoptosis	24
Costimulatory molecules	24
Cell cycle	23
Complement	23
Cell activation	19
Major histocompatibility complex	15
Toll-like receptor	10
Cytotoxicity	08
Cell proliferation	03
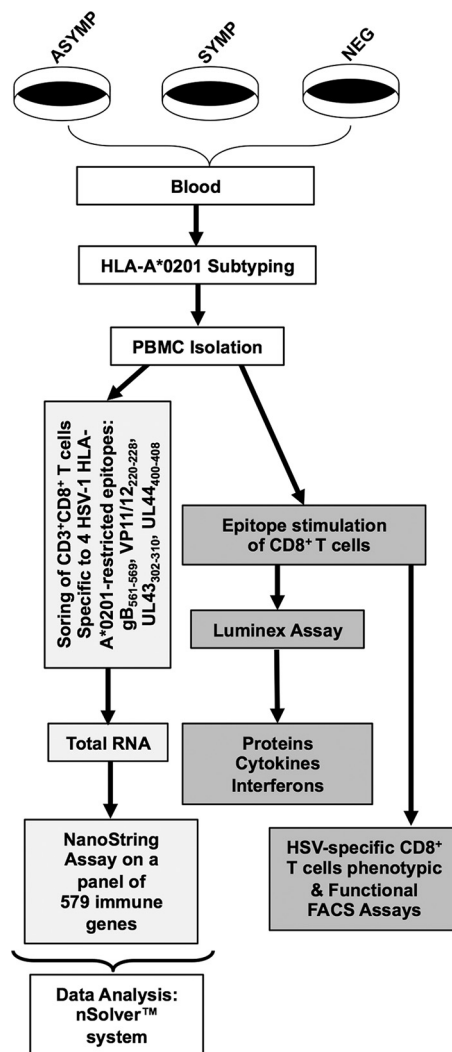
FIG 1 Experimental design. CD8+ T cells specific to four HLA-A*0201-restricted epitopes (gB$_{561-567}$, VP11/12$_{220-228}$, UL43$_{302-310}$, and UL44$_{400-408}$) identified from HSV-1 envelope, tegument, and regulatory proteins were sorted using correspondent tetramers from HLA-A*0201-positive ASYMP ($n = 10$), SYMP ($n = 10$), and seronegative ($n = 10$) individuals. Total mRNAs were extracted from each clone of CD8+ T cells, and NanoString technology was used to compare the levels of expression of 579 immune genes. Supernatants were collected on days 2 and 14 after stimulation with gB$_{561-567}$, VP11/12$_{220-228}$, UL43$_{302-310}$, and UL44$_{400-408}$ or peptide and the amounts of produced cytokines were determined using Luminex. The expression levels of different cytokine receptors, CD107, GzmB, GzmK, PFN, IFN-γ, and Ki-67, were determined by FACS on tetramer-gated HSV-1 epitope-specific CD8+ T cells.

As illustrated in Fig. 1, blood-derived CD8+ T cells, specific to four HLA-A*0201-restricted epitopes from various HSV-1 proteins, were enriched by high-purity fluorescence activated cell sorting (FACS) from well-characterized cohorts of gender- and age-matched (i) HLA-A*0201-positive SYMP individuals ($n = 10$), (ii) HLA-A*0201-positive ASYMP individuals ($n = 10$), and (iii) HLA-A*0201-positive seronegative NEG individuals ($n = 10$). We used HLA-A*0201/tetramers specific to HLA-A*0201-restricted epitopes selected from the HSV-1 membrane glycoprotein B (gB$_{561-569}$) and the tegument proteins VP11/12 (also known as UL46) (VP11-12$_{220-228}$), UL43 (UL43$_{302-310}$), and UL44 (UL44$_{400-408}$). RNA samples were isolated from half of HSV epitope-specific CD8+ T cells, which were sorted from 10 SYMP versus 10 ASYMP individuals as well as from 10 NEG controls, using HLA-A*0201/tetramers specific to each of the 4 HLA-A*0201-restricted epitopes, mentioned above. The customized panel of 579 immune genes was hybridized to total RNAs using the high-throughput digital NanoString nCounter system, which accurately quantifies the level of gene expression from the HSV epitope-
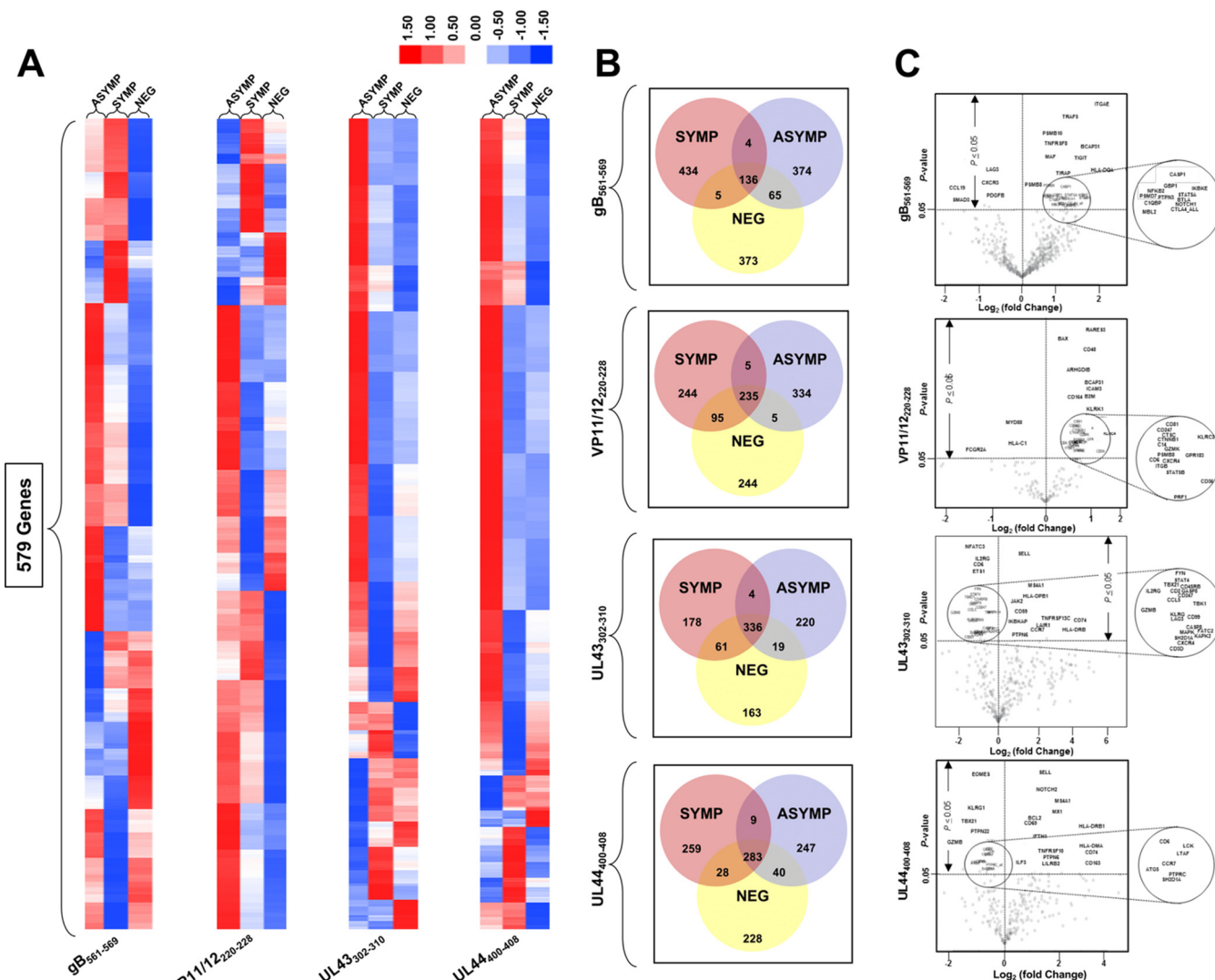
FIG 2 Profile of immune genes expressed by HSV-specific CD8+ T cells from SYMP versus ASYMP individuals. (A) Heat map of the gene expression profiles detected from HSV-1 $gB_{561-567}$-, $VP11/12_{220-228}$-, $UL43_{302-310}$-, and $UL44_{400-408}$-specific CD8+ T cells isolated from ASYMP, SYMP, and NEG individuals. The heat map was generated by nSolver software, with the grouped values generated by taking the mean of the gene expression levels from 10 ASYMP, 10 SYMP, and 10 NEG individuals. The heat map illustrates upregulation (red) and downregulation (blue) of 579 immune genes in HSV-specific CD8+ T cells specific to four HSV-1 epitopes. (B) Venn diagram depicting the average numbers of genes differentially expressed on tetramer-gated $gB_{561-567}$-, $VP11/12_{220-228}$-, $UL43_{302-310}$-, and $UL44_{400-408}$-specific CD8+ T cells from 10 NEG, 10 ASYMP, and 10 SYMP individuals. (C) Volcano plot showing the immune genes that are significantly ($P < 0.05$) different in CD8+ T cells, specific to $gB_{561-567}$, $VP11/12_{220-228}$, $UL43_{302-310}$, and $UL44_{400-408}$ epitopes, sorted from 10 ASYMP individuals versus 10 SYMP individuals. Each dot represents differential gene expression. The circles are meant to highlight clusters of genes. Results are representative of those from two independent experiments in each individual. The indicated P values, calculated using unpaired t test, show statistical significance between SYMP and ASYMP individuals.
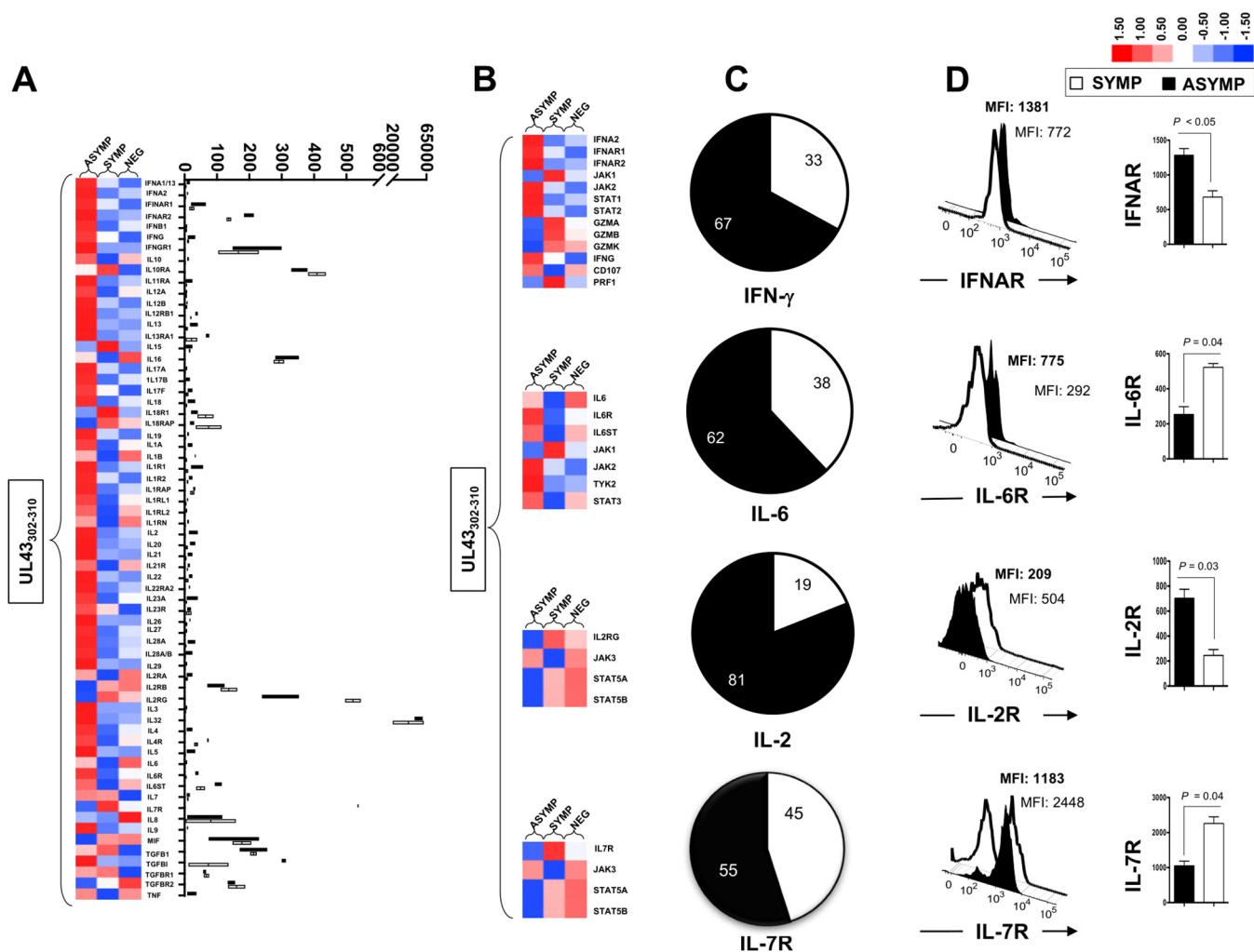
specific CD8+ T cells from SYMP, ASYMP, and NEG individuals. The other half of HSV epitope-specific CD8+ T cells were stimulated *in vitro* with $gB_{561-569}$, $VP11-12_{220-228}$, $UL43_{302-310}$, or $UL44_{400-408}$ epitope. The amounts of cytokines produced were detected by Luminex assay, and the levels of expression of cytokine receptors were detected by FACS.

Overall, there was a high level of gene expression of HSV-1 $gB_{561-569}$-, $VP11-12_{220-228}$-, $UL43_{302-310}$-, and $UL44_{400-408}$-specific CD8+ T cells from ASYMP compared to SYMP individuals and to healthy NEG controls (Fig. 2). The nCounter 579 immune gene panel substratified HSV-1 $gB_{561-569}$-, $VP11-12_{220-228}$-, $UL43_{302-310}$-, and $UL44_{400-408}$-specific CD8+ T cells from SYMP and ASYMP individuals into two subsets with statistically significant differences in the levels of gene expression ($P = 0.05$) (Fig. 2).

Differential gene expression was performed on the basis of grouped mean data for 10 ASYMP, 10 SYMP, and 10 seronegative individuals. The gene expression profiles evident from the heat map for HSV-1 $UL43_{302\text{-}310}$, $gB_{561\text{-}567}$, $VP11/12_{220\text{-}228}$, and $UL44_{400\text{-}408}$ epitope-specific $CD8^+$ T cells showed the upregulation of genes associated with various pathways including expansion/survival, chemokines/cytokines, type I interferons (IFNs), JAK/STAT signaling pathway, transcription factor, costimulatory molecules, adhesion molecules, cell differentiation, apoptosis, cytotoxicity, and cell proliferation among ASYMP individuals (Fig. 2A). The average numbers of genes differentially expressed on tetramer-gated $UL43_{302\text{-}310}$, $gB_{561\text{-}567}$, $VP11/12_{220\text{-}228}$, and $UL44_{400\text{-}408}$ epitope-specific $CD8^+$ T cells, depicted in the Venn diagram in Fig. 2B, confirmed this immune gene upregulation from 10 ASYMP compared 10 SYMP individuals. Of the 579 immune genes tested, up to 239 were upregulated/downregulated in HSV-1 $UL43_{302\text{-}310}$ epitope-specific $CD8^+$ T cells from ASYMP individuals, while 239 different genes were upregulated/downregulated in $CD8^+$ T cells from SYMP individuals. The levels of 340 genes were similar in $CD8^+$ T cells that shared the same HSV-1 $UL43_{302\text{-}310}$ epitope specificity from ASYMP and SYMP individuals. Our volcano plot showed that the most different immune genes in $CD8^+$ T cells, specific to $UL43_{302\text{-}310}$, $gB_{561\text{-}567}$, $VP11/12_{220\text{-}228}$, and $UL44_{400\text{-}408}$ epitopes, sorted from ASYMP individuals are for expansion/survival chemokines/cytokines, type I IFNs, the JAK/STAT signaling pathway, transcription factor, costimulatory molecules, adhesion molecules, cell differentiation, apoptosis, cytotoxicity, and cell proliferation pathways (Fig. 2C). The most notable was the low expression of Tcf7 (TCF1) in $CD8^+$ T cells from SYMP individuals compared to the high expression of Tcf7 in $CD8^+$ T cells from ASYMP individuals and the critical role of this transcription factor in the generation of these cells. Thus, many aspects of the transcriptional programs of these two cell types are distinct. Similar results were obtained in $CD8^+$ T cells specific to the remaining 3 epitopes: $gB_{561\text{-}569}$, $VP11\text{-}12_{220\text{-}228}$, and $UL44_{400\text{-}408}$ (Fig. 2). Together, these results suggest an upregulation of many immune genes in HSV-specific $CD8^+$ T cells from ASYMP individuals compared to HSV-specific $CD8^+$ T cells from SYMP individuals.

The HSV-specific $CD8^+$ T cells from ASYMP individuals expressed a unique gene signature characterized by higher levels of genes for type I IFNs, expansion/survival cytokines, and the JAK/STAT pathway. We next determined whether specific genes for interferons, cytokines, and JAK/STAT signatures can be found in ASYMP versus SYMP individuals. Blood-derived $CD8^+$ T cells were sorted using FACS from sex- and age-matched HLA-A*0201-positive SYMP patients ($n = 10$), ASYMP patients ($n = 10$), and 10 seronegative individuals using tetramers specific to the HSV-1 $gB_{561\text{-}569}$, $VP11\text{-}12_{220\text{-}228}$, $UL44_{400\text{-}408}$, and $UL43_{302\text{-}310}$ epitopes, as described above. Total mRNAs were extracted, and NanoString assay was used to compare the levels of expression of genes for JAK/STAT, interferons, cytokines, and their receptors.

Our results indicate that regardless of the HSV-1 epitopes, a unique gene signature characterized by higher levels of genes for type I IFNs, expansion/survival cytokines (interleukin 2 [IL-2], IL-4, IL-6, IL-6ST, IL-6R, and IL-7) and the JAK/STAT pathway (e.g., JAK2, JAK3, STAT3, and STAT5B) were detected in HSV-specific $CD8^+$ T cells from ASYMP than from SYMP individuals. A heat map illustrating upregulated (red) and downregulated (blue) genes in HSV-1 $UL43_{302\text{-}310}$-specific $CD8^+$ cells from the grouped mean of 10 ASYMP, 10 SYMP, and 10 seronegative individuals is shown in Fig. 3A (left side). The transcriptional profiles in $UL43_{302\text{-}310}$-specific $CD8^+$ T cells from ASYMP individuals had a unique gene signature characterized by higher levels of genes for IFN-I, IL-6, IL-2, and IL-7 (Fig. 3A, right side). The average frequencies of expression of genes calculated across all samples of $CD8^+$ T cells from 10 SYMP and 10 ASYMP individuals confirmed higher levels of expression of IFN-I, IL-6, IL-2, and IL-7 genes in ASYMP individuals (Fig. 3A, right side). The representative heat maps also indicate an upregulation of JAK/STAT genes in HSV-1 $UL43_{302\text{-}310}$-specific $CD8^+$ T cells from ASYMP individuals (Fig. 3B). Specifically, the HSV-specific $CD8^+$ T cells derived from ASYMP individuals expressed high levels of JAK2, JAK3, STAT3, and STAT5 genes.

FIG 3 Gene profiles of cytokines and cytokine receptors in HSV-specific CD8+ T cells from SYMP versus ASYMP individuals. Blood-derived CD8+ T cells were sorted using FACS from age-matched HLA-A*0201-positive SYMP patients ($n = 10$), ASYMP patients ($n = 10$), and 10 seronegative individuals using tetramers specific to HSV-1 UL43$_{302-310}$ epitope. Total mRNAs were extracted, and NanoString assay was used to compare the levels of expression of cytokines and cytokine receptor genes. (A) Transcriptional profiles of cytokine and cytokine receptors in CD8+ T cells specific to UL43$_{302-310}$. A representative heat map illustrating genes that are upregulated (red) or downregulated (blue) in HSV-1 UL43$_{302-310}$-specific CD8+ cells from the grouped mean of 10 seronegative, 10 ASYMP, and 10 SYMP individuals is shown on the left. Average frequencies of expression of genes calculated across all samples of CD8+ T cells from 10 SYMP and 10 ASYMP individuals are shown on the right. The results are representative of those from two independent experiments in each individual. (B) Representative heat maps illustrating transcriptional profiles of genes involved in IFN-γ, IL-6, IL-2, and IL-7 signaling pathways in HSV-1 UL43$_{302-310}$-specific CD8+ T cells. (C) Summary pie charts showing the average amounts of IFN-γ, IL-6, IL-2, and IL-7 cytokines produced by CD8+ T cells as detected by Luminex and intracellular FACS assays 2 days after UL43$_{302-310}$ peptide restimulation. The numbers inside each pie chart show the average frequencies of CD8+ T cells producing each cytokine from 10 SYMP and 10 ASYMP individuals. (D) Expression levels of receptors for IFN-γ, IL-6, IL-2, and IL-7 were detected by FACS on tetramer-gated CD8+ T cells. The representative FACS data (left) with bold numbers on the top of each histogram represent MFIs depicting the level of expression on ASYMP CD8+ T cells. The average MFIs for the levels of cytokines on tetramer-gated UL43$_{302-310}$ epitope-specific CD8+ T cells from 10 ASYMP and 10 SYMP individuals are also shown (right). Acquisition of samples was performed on a BD LSRII flow cytometer, and FlowJo software was used for data analysis. The results are representative of those from two independent experiments in each individual. The P values were calculated using the unpaired t test and show statistical significance between SYMP and ASYMP individuals. Asterisks indicate the genes with most significant differences in expression between SYMP and ASYMP individuals.

Larger amounts of IFN-γ, IL-6, IL-2, and IL-7 produced by CD8+ T cells from ASYMP individuals were also confirmed by Luminex assay following UL43$_{302-310}$ peptide restimulation (Fig. 3C). The numbers inside each pie chart indicate average frequency of CD8+ T cells producing each cytokine as detected by intracellular FACS staining from 10 SYMP and 10 ASYMP individuals. Similar to their corresponding cytokines, higher levels of expression of IFN, IL-6, IL-2, and IL-7 receptors were detected by FACS on UL43$_{302-310}$ tetramer-gated CD8+ T cells from ASYMP than from SYMP individuals (Fig. 3D). The representative FACS data with bold numbers on the top of each histogram represent median fluorescence intensities (MFIs), revealing significantly high levels of
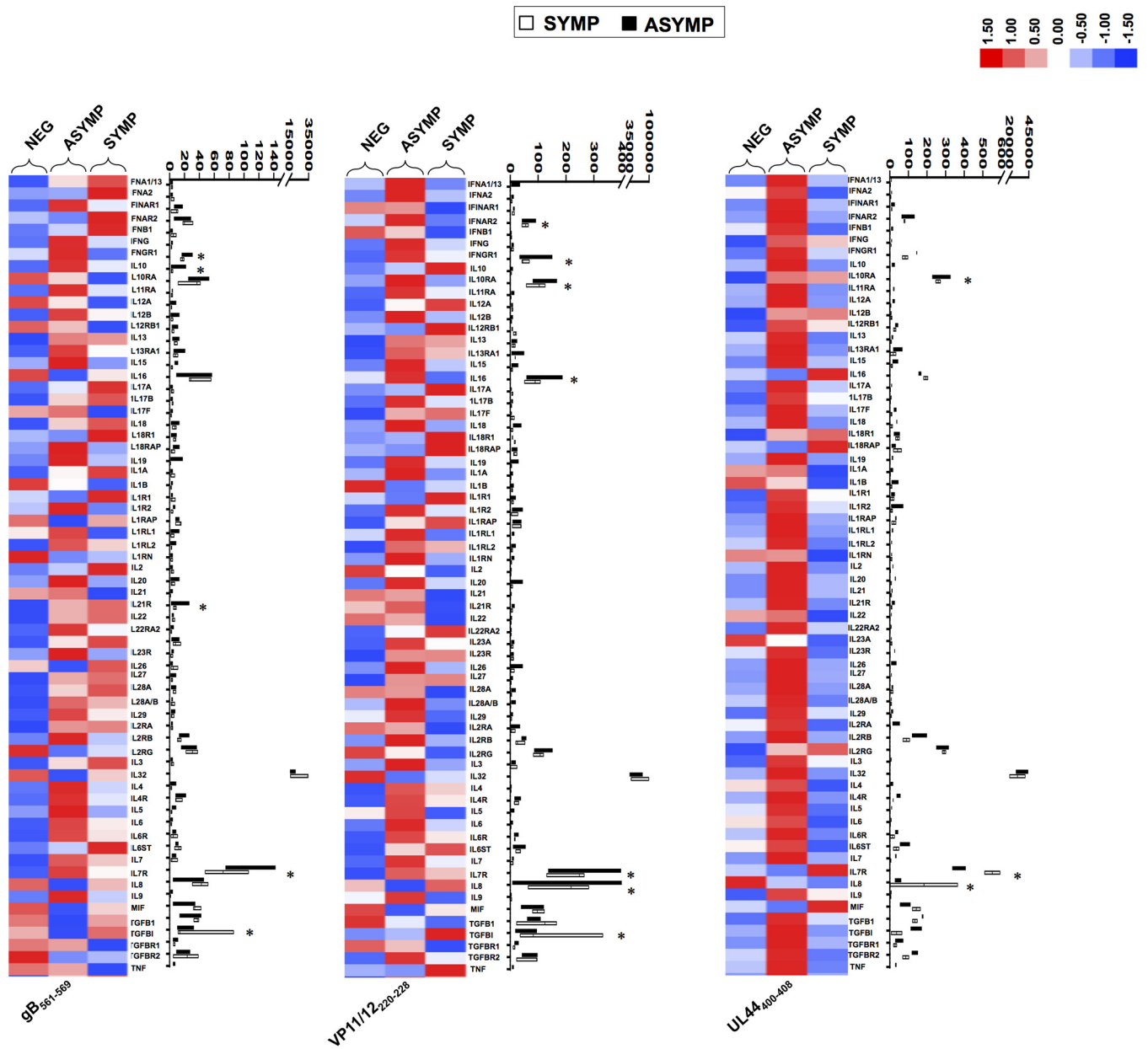
FIG 4 Gene profiles of cytokines and chemokine receptors in HSV-1 gB$_{561-567}$, VP11/12$_{220-228}$, and UL44$_{400-408}$ peptide-specific CD8$^+$ T cells from SYMP versus ASYMP individuals. Blood-derived CD8$^+$ T cells were sorted using FACS from age-matched HLA-A*0201-positive SYMP ($n = 10$) and ASYMP patients ($n = 10$) and seronegative subjects ($n = 10$) using tetramers specific to the HSV-1 gB$_{561-567}$, VP11/12$_{220-228}$, and UL44$_{400-408}$ epitopes, respectively. Total mRNAs were extracted, and NanoString assay was used to compare the expression levels of cytokines and chemokine receptor genes. Shown are representative heat maps illustrating genes that were upregulated (red) or downregulated (blue) in CD8$^+$ T cells specific to gB$_{561-567}$, VP11/12$_{220-228}$, and UL44$_{400-408}$ epitopes (left); average frequencies of gene expression calculated across all samples of CD8$^+$ T cells from 10 SYMP and 10 ASYMP are shown on the right. Results are representative of those from two independent experiments in each individual. Asterisks indicate the genes with most significant differences in expression between SYMP and ASYMP individuals.

expression of IFN-γ, IL-6, IL-2, and IL-7 receptors on ASYMP CD8$^+$ T cells (Fig. 3D, left side). Average MFIs for the levels of IFN-γ, IL-6, IL-2, and IL-7 receptors on tetramer-gated UL43$_{302-310}$ epitope-specific CD8$^+$ T cells from 10 ASYMP and 10 SYMP individuals are shown ($P < 0.05$) (Fig. 3D, right side). Similarly, higher levels of IFN-I, IL-6, IL-2, and IL-7 cytokines and of JAK/STAT pathways specific genes were detected in gB$_{561-569}$, VP11-12$_{220-228}$, and UL44$_{400-408}$ epitope-specific CD8$^+$ T cells from ASYMP individuals than from SYMP individuals (Fig. 4).

Frequent HSV-specific CD8$^+$ T$_{EM}$ cells detected in asymptomatic individuals compared to symptomatic individuals. We next investigated whether the same or

different frequencies of HSV-specific memory CD8+ T_{EM} and T_{CM} cells could be detected in age- and sex-matched HLA-A*0201-positive SYMP versus ASYMP individuals. Freshly isolated peripheral blood-derived CD3+ CD8+ T cells were gated on CD8+ T cells specific to the HSV-1 $gB_{561-569}$, $VP11-12_{220-228}$, $UL44_{400-408}$, and $UL43_{302-310}$ epitopes. Using HLA-A*02:01-specific tetramers/anti-CD8 monoclonal antibodies (MAbs), we compared the frequencies of CD8+ T_{CM} and CD8+ T_{EM} cells specific to the above-mentioned HLA-A*0201-restricted epitopes from peripheral blood of 10 HLA-A*02:01-positive, HSV-1-seropositive ASYMP and 10 HLA-A*02:01-positive, HSV-1-seropositive SYMP individuals. The low frequencies of peripheral blood mononuclear cell (PBMC)-derived HSV-specific CD8+ T cells complicated direct *ex vivo* detection of CD8+ T_{CM} and CD8+ T_{EM} cells with tetramers using a typical number of PBMCs ($\sim 10^6$), and a prior expansion of CD8+ T cells by HSV-1 or peptide stimulation in an *in vitro* culture will hamper a reliable determination of the frequency of HSV epitope-specific CD8+ T cells. We therefore opted to measure the frequencies of HSV epitope-specific CD8+ T cells *ex vivo* using a large number of PBMCs ($\sim 10 \times 10^6$) per tetramer/CD8 MAb panel.

Figure 5A shows gating strategies used to characterize the phenotype and function of CD8+ T cells specific to $gB_{561-567}$, $VP11/12_{220-228}$, $UL43_{302-310}$, and $UL44_{400-408}$ epitopes. Figure 5B shows a representative FACS contour plot depicting higher frequencies of CD44high CD62Llow CD8+ T_{EM} cells specific to $gB_{561-567}$, $VP11/12_{220-228}$, $UL43_{302-310}$, and $UL44_{400-408}$ epitopes detected from two SYMP individuals (left contour plots) versus two ASYMP individual (right contour plots). Figure 5C shows an average higher frequency (left graphs) and absolute numbers (right graphs) of epitope-specific CD8+ T_{EM} cells detected from 10 ASYMP than from 10 SYMP individuals. Thus, ASYMP individuals had significantly higher percentages of CD62Llow CD44high CD8+ T_{EM} cells specific to $gB_{561-567}$, $VP11/12_{220-228}$, $UL43_{302-310}$, and $UL44_{400-408}$ epitopes than did SYMP individuals ($P < 0.05$). In contrast, we consistently detected significantly higher percentages of HSV epitope-specific CD62Lhigh CD44high CD8+ T_{CM} cells in SYMP individuals than in ASYMP individuals ($P < 0.05$).

Altogether, the results of the phenotypic study revealed a clear difference in the phenotypes of HSV-specific memory CD8+ T cells in SYMP versus ASYMP individuals irrespective of the HSV-1 epitope used. Thus, blood-derived HSV-specific memory CD8+ T cells from HSV-1-seropositive SYMP versus ASYMP individuals are categorized into two major phenotypically distinct HSV-specific CD8+ T_{CM} cell and HSV-specific CD8+ T_{EM} cell subpopulations, respectively. These results suggest that (i) by maintaining high frequencies of the "experienced" HSV-specific CD8+ T_{EM} cells, the ASYMP individuals should be better protected against HSV-1 infection, reactivation, and/or subsequent herpetic disease, and (ii) at a subsequent pathogen encounter (e.g., following HSV-1 reactivation from latency), the ASYMP individuals, but not SYMP individuals, would mount much faster and stronger protective HSV-specific CD8+ T_{EM} cell responses, allowing a better clearance of herpesvirus infection and disease.

Asymptomatic individuals develop multifunctional HSV-specific CD8+ T cells. We next compared the functions of HSV epitope-specific effector CD8+ T cells from SYMP versus ASYMP individuals. Because the frequency of $gB_{561-569}$, $VP11/12_{220-228}$, and $UL44_{400-408}$ epitopes is relatively low, the functional studies were focused only on the immunodominant $UL43_{302-310}$ epitope.

We first compared the proliferative responses using Ki-67 and determined the ability of $UL43_{302-310}$ epitope-specific CD8+ T cells from SYMP versus ASYMP individuals to produce IFN-γ and express degranulation marker CD107a/b following *in vitro* stimulation with $UL43_{302-310}$ peptide. Freshly isolated CD8+ T cells from SYMP and ASYMP individuals were stimulated *in vitro* for 2 days with the $UL43_{302-310}$ peptide, as described in Materials and Methods. The percentages and numbers of IFN-γ+ CD8+ T and CD107a/b+ CD8+ T cells from SYMP and ASYMP individuals were compared by intracellular FACS staining.

Significantly higher percentages of $UL43_{302-310}$-specific CD8+ T cells from ASYMP individuals showed an upregulation of Ki-67 ($\sim 3.5\%$), indicative of increased prolifer-
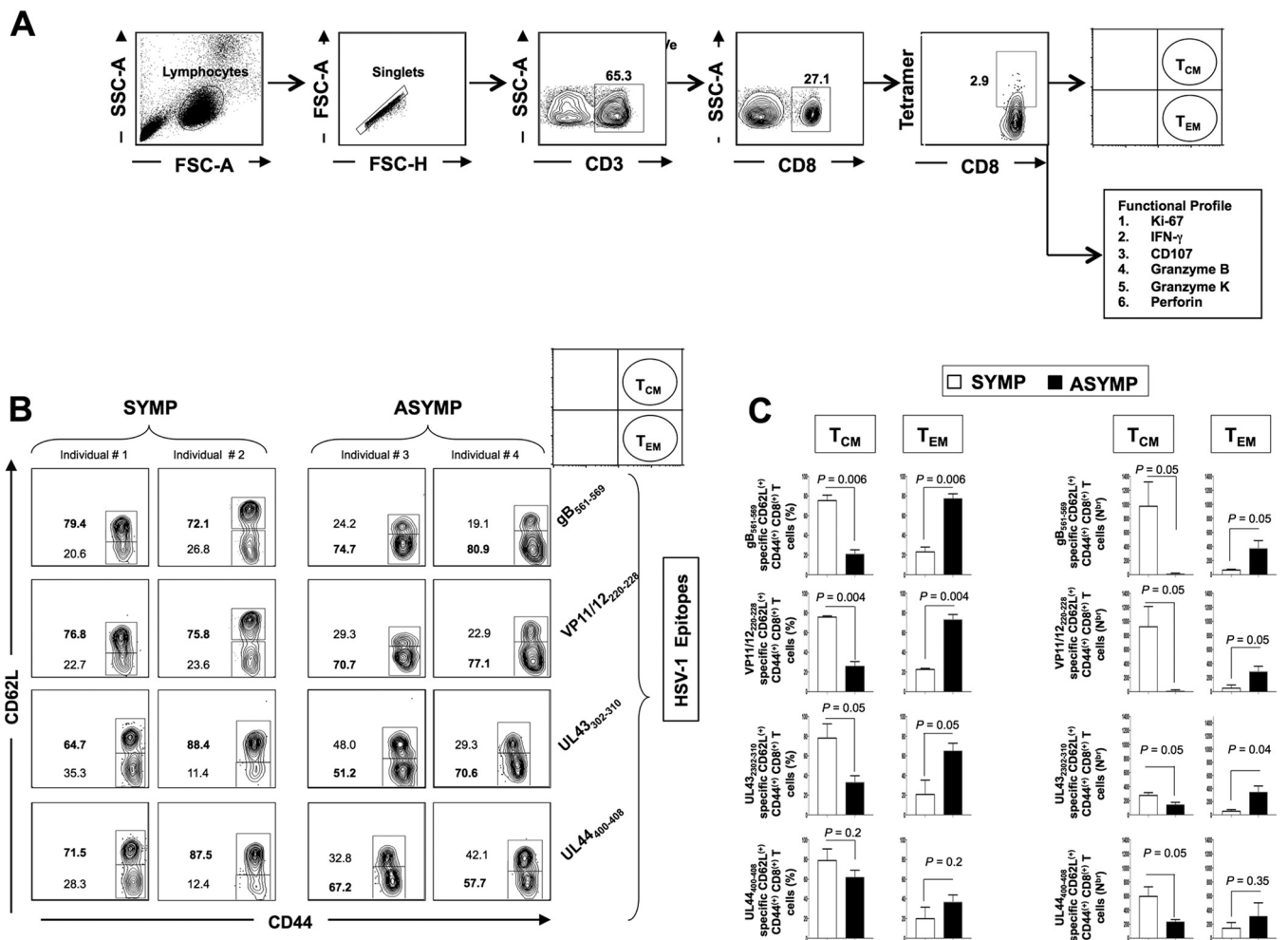
FIG 5 Comparison of the frequency of HSV-1-specific CD44^{high} CD62L^{low} CD8^{+} T$_{EM}$ and CD44^{high} CD62L^{high} CD8^{+} T$_{CM}$ cells in SYMP versus ASYMP individuals. PBMCs ($\sim$10 $\times$ 10^6) derived from 10 HLA-A*02:01-positive, HSV-1-seropositive ASYMP individuals and from 10 HLA-A*0201-positive, HSV-1-seropositive SYMP individuals were analyzed *ex vivo* by FACS for the frequency of T$_{CM}$ and T$_{EM}$ CD8^{+} T cells specific to four HSV-1 epitopes: gB$_{561-567}$, VP11/12$_{220-228}$, UL43$_{302-310}$, and UL44$_{400-408}$. (A) Gating strategies used to characterize the phenotype and function of CD8 T cells specific to gB$_{561-567}$, VP11/12$_{220-228}$, UL43$_{302-310}$, and UL44$_{400-408}$ epitopes. (B) Representative FACS contour plot depicting the frequencies of CD44^{high} CD62L^{high} CD8^{+} T$_{CM}$ cells and CD44^{high} CD62L^{low} CD8^{+} T$_{EM}$ cells specific to gB$_{561-567}$, VP11/12$_{220-228}$, UL43$_{302-310}$, and UL44$_{400-408}$ epitopes respectively detected from SYMP individuals 1 and 2 (2 left contour plots) and ASYMP individuals 3 and 4 (2 right contour plots). (C) Average percentages (left graphs) and absolute numbers (right graphs) of epitope-specific T$_{CM}$ and T$_{EM}$ cells detected from 10 ASYMP and 10 SYMP individuals. Samples were acquired on a BD LSRII flow cytometer, and data analysis was performed using FlowJo software. Results are representative of those from two independent experiments in each individual. The indicated P values, calculated using unpaired t test, show statistical significance between SYMP and ASYMP individuals.

ation of HSV-specific CD8^{+} T cells, than from SYMP individuals ($\sim$1.2) (Fig. 6A and B, left) ($P = 0.002$). Moreover, significantly higher percentages of UL43$_{302-310}$-specific CD8^{+} T cells producing IFN-γ were detected in ASYMP individuals ($\sim$28.2%) than in SYMP individuals ($\sim$13.7%) (Fig. 6A and B, middle) ($P = 0.001$). We also observed significantly higher percentages of UL43$_{302-310}$-specific CD8^{+} T cells expressing CD107$^{a/b}$ in ASYMP individuals ($\sim$14.1%) than in SYMP individuals, suggesting higher HSV-specific cytotoxic function of CD8^{+} T cells from ASYMP individuals ($\sim$6.8%) (Fig. 6A and B, right) ($P = 0.001$). Similar trends for Ki-67, IFN-γ, and CD107$^{a/b}$ were noted when CD8^{+} T cells from SYMP and ASYMP individuals were stimulated with gB$_{561-569}$, VP11/12$_{220-228}$, and UL44$_{400-408}$ epitopes (data not shown).

We then compared the expressions of granzyme B (GzmB), granzyme K (GzmK), and perforin (PFN) on gated UL43$_{302-310}$-specific CD8^{+} T cells from 10 SYMP and 10 ASYMP individuals (Fig. 6C and D). We found significantly higher levels of GzmB, GzmK, and PFN expressed on UL43$_{302-310}$-specific CD8^{+} T cells from ASYMP than from SYMP individuals, suggesting a positive correlation of strong HSV-specific CD8^{+} T-cell cyto-
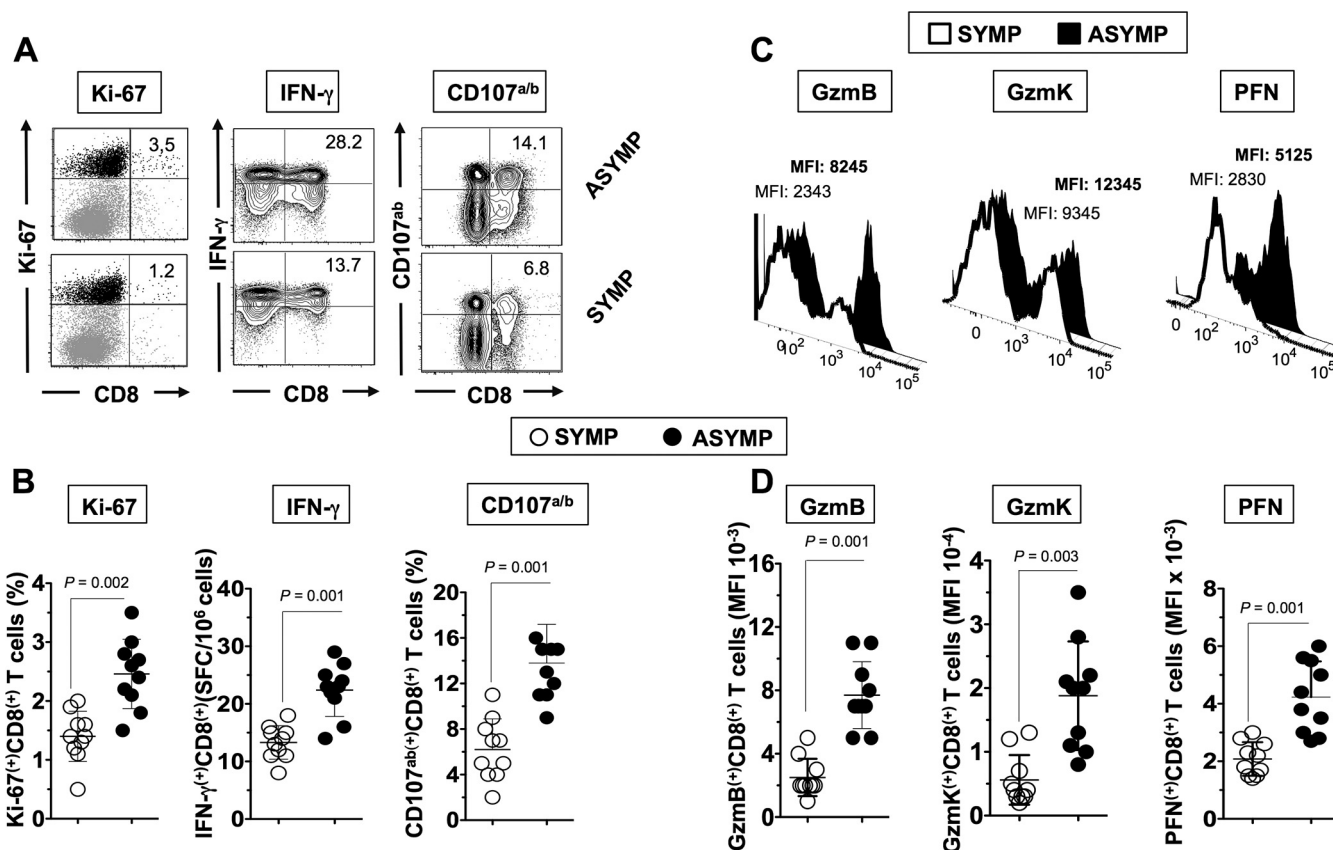
FIG 6 Comparison of the proliferative, cytokine production and cytotoxicity functions of HSV-1 epitope-specific CD8+ T cells derived from SYMP versus ASYMP individuals: (A) Representative FACS data of the percentages of UL43$_{302-310}$-epitope specific Ki-67+ CD8+ T cells, IFN-γ+ CD8+ T cells, and CD107$^{a/b+}$ CD8+ T cells from one ASYMP individual (top three plots) and one SYMP individual (bottom three plots). (B) Average percentages of UL43$_{302-310}$-epitope-specific Ki-67+ CD8+ T cells, IFN-γ+ CD8+ T cells, and CD107$^{a/b+}$ CD8+ T cells detected from 10 SYMP and 10 ASYMP individuals. (C) Representative FACS data on the expression levels of GzmB, GzmK, and PFN on UL43$_{302-310}$ tetramer-gated CD8+ T cells. The numbers at the top of each histogram represent MFIs, depicting the level of expression of each cytotoxic molecule in SYMP versus ASYMP individuals. (D) Average levels of GzmB, GzmK, and PFN detected on UL43$_{302-310}$ tetramer-gated CD8+ T cells from 10 ASYMP and 10 SYMP individuals. Results are representative of those from two independent experiments, and the indicated P values, calculated using unpaired t test, show statistical significance between SYMP and ASYMP individuals.

toxic responses with protection seen in ASYMP ocular herpes ($P < 0.003$) (Fig. 6C and D). Similar trends were noted comparing CD8+ T cells specific to gB$_{561-569}$, VP11/12$_{220-228}$, and UL44$_{400-408}$ epitopes in SYMP and ASYMP individuals (data not shown).

Together, these results indicate that HSV-specific effector CD8+ T cells from ASYMP individuals are multifunctional. In contrast, HSV-specific effector CD8+ T cells from SYMP individuals are mostly monofunctional. The significantly higher percentages of cytotoxic HSV-specific Ki-67+ IFN-γ+, and CD107$^{a/b+}$ CD8+ T cells detected in ASYMP individuals make them better prepared to mount protective response against recurrent herpes.

Higher levels of cytokines and cytokine receptors expressed by HSV-specific CD8+ T cells from ASYMP than from SYMP individuals. The levels of cytokines (detected by Luminex) and cytokine receptor proteins (detected by FACS) were compared in blood-derived gB$_{561-567}$-, VP11/12$_{220-228}$-, and UL44$_{400-408}$-specific CD8+ T cells from age-matched HLA-A*0201-positive SYMP ($n = 10$) and ASYMP ($n = 10$) patients. As shown in Fig. 7A, larger amounts of IFN-γ, IL-6, IL-7, and IL-2 cytokines were produced by CD8+ T cells from ASYMP individuals following a 2-day stimulation with either gB$_{561-567}$, VP11/12$_{220-228}$, or UL44$_{400-408}$ peptide. The number inside each pie chart shows the average frequency of CD8+ T cells producing each cytokine from 10 SYMP and 10 ASYMP individuals. Similar to the case with the cytokines, as shown in Fig. 7B, higher levels of expression of receptors for IFN, IL-6, IL-7, and IL-2 were also detected by FACS on gB$_{561-567}$, VP11/12$_{220-228}$, and UL44$_{400-408}$ tetramer-gated CD8+ T
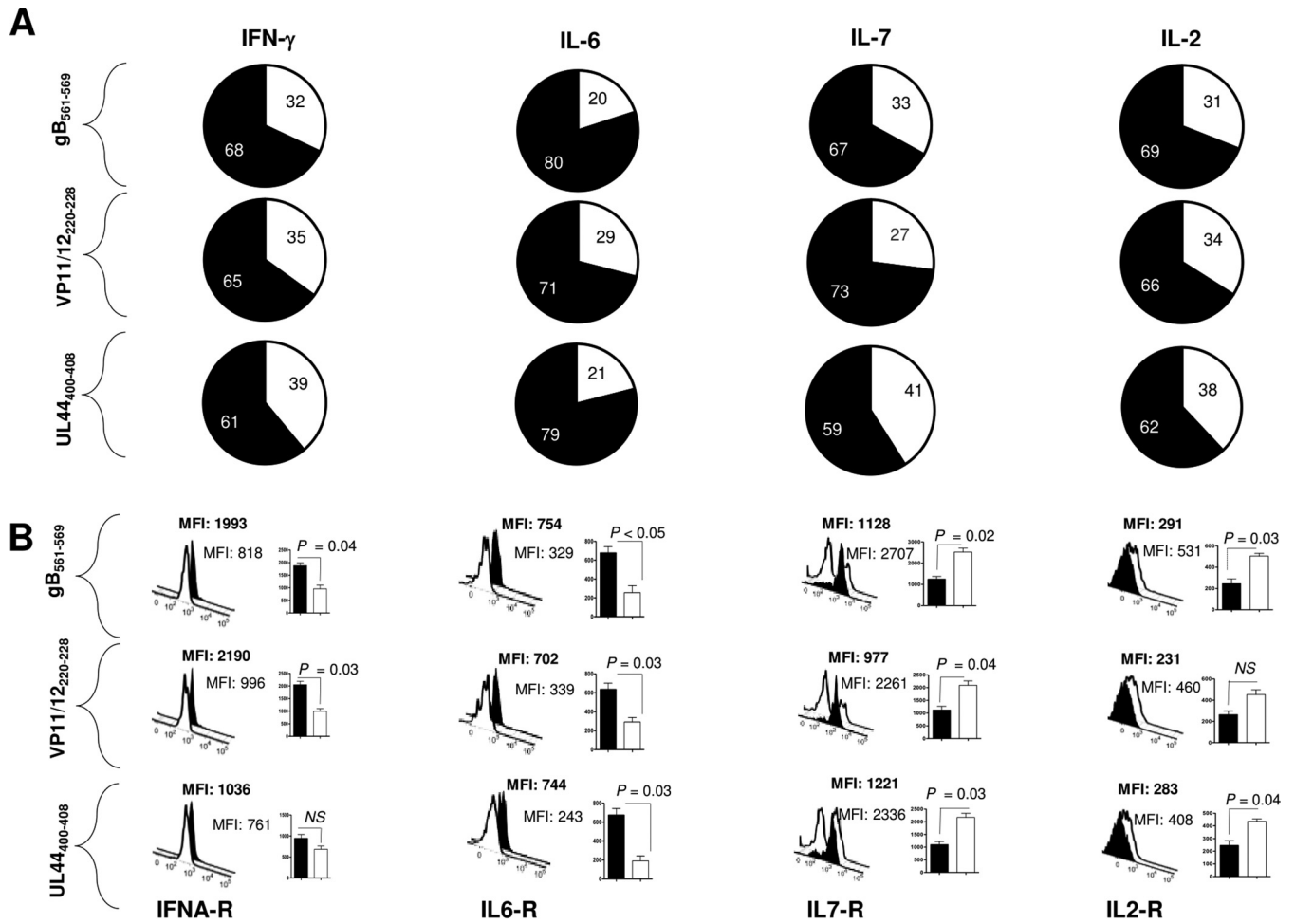
FIG 7 Profiles of cytokines and cytokine receptors in HSV-specific CD8$^+$ T cells from SYMP versus ASYMP individuals. Cytokines and cytokine receptor protein levels were compared in blood-derived gB$_{561-567}$, VP11/12$_{220-228}$, and UL44$_{400-408}$-specific CD8 T cells from age-matched HLA-A*0201-positive SYMP ($n = 10$) and ASYMP patients ($n = 10$). (A) Summary pie charts showing the average amounts of IFN-γ, IL-6, IL-7, and IL-2 cytokines produced by CD8$^+$ T cells and detected by Luminex assay 2 days after stimulation with either gB$_{561-567}$, VP11/12$_{220-228}$, or UL44$_{400-408}$ peptide. The number inside each pie chart shows the average frequency of CD8$^+$ T cells producing each cytokine from 10 SYMP and 10 ASYMP individuals. (B) Expression levels of receptors for IFN, IL-6, IL-7, and IL-2 detected by FACS on gB$_{561-567}$, VP11/12$_{220-228}$, and UL44$_{400-408}$ tetramer-gated CD8$^+$ T cells. Shown are representative FACS data (left), with bold numbers at the top of each histogram represent MFIs, depicting the level of expression on ASYMP CD8$^+$ T cells, and average MFIs for the levels of cytokine receptors on respective tetramer-gated CD8$^+$ T cells from 10 ASYMP and 10 SYMP individuals (right). Samples were acquired on a BD LSRII flow cytometer, and data analysis was performed using FlowJo software. Results are representative of those from two independent experiments in each individual. The indicated P values, calculated using the unpaired t test, show statistical significance between SYMP and ASYMP individuals.

cells from ASYMP individuals than from SYMP individuals. The representative FACS data (Fig. 7B, left) with bold numbers on the top of each histogram represent MFIs, depicting the high level of expression on CD8$^+$ T cells from ASYMP individuals. The FACS data (Fig. 7B, right) revealed average MFIs for the levels of cytokine receptors on tetramer-gated UL43$_{302-310}$ epitope-specific CD8$^+$ T cells from 10 ASYMP and 10 SYMP individuals. Similar to the results above, these data confirm higher levels of cytokines and cytokine receptors expressed by HSV-specific CD8$^+$ T cells from ASYMP than from SYMP individuals.

DISCUSSION

In the present study, we compared the genomic, phenotypic, and functional features of memory CD8$^+$ T cells that share the same HSV-1 epitope specificities but were from HSV-1-seropositive symptomatic (SYMP) and asymptomatic (ASYMP) individuals. Unlike SYMP individuals, ASYMP individuals do not experience any apparent recurrent herpetic disease, likely because their T cells (among other effectors of immunity) control the infection and/or disease to a clinically undetectable level (reviewed in reference 8).

We report striking genomic, phenotypic, and functional differences of CD8+ T cells from SYMP and ASYMP individuals, including the following: (i) a significant divergence in immune gene signatures of CD8+ T cells that, although they shared the same HSV-1 epitope specificity, were derived from either "protected" ASYMP individuals or from "nonprotected" SYMP individuals, and (ii) regardless of the epitope specificities, CD8+ T$_{EM}$ cells from all ASYMP individuals expressed a unique gene signature consistent with an active Janus kinase/signal transducer and activator of transcription (JAK/STAT) pathway, type I interferon (IFN), and cytokines involved in T-cell survival and expansion (e.g., *JAK2*, *STAT3*, *STAT5B*, *IL-2*, *IL-4*, *IL-6*, *IL-6ST*, *IL-6R*, and *IL-7*). In contrast, HSV-specific CD8+ T$_{CM}$ cells derived from SYMP individuals expressed low levels of *JAK/STAT* and *IFN-I*, survival/expansion cytokine genes. Accordingly, HSV-specific CD8+ T cells from ASYMP individuals were polyfunctional CD62L^{low} CD44^{high} CD8+ T$_{EM}$ cells. In contrast, HSV-specific CD8+ T$_{CM}$ cells from SYMP individuals were mostly monofunctional CD62L^{high} CD44^{high} CD8+ T$_{CM}$ cells. The findings have profound implications in the development of T-cell-based immunotherapeutic vaccines. Moreover, since the immune signatures associated with immune protection in ASYMP individuals (versus immunopathology in SYMP individuals) were identified on circulating peripheral blood-derived T cells, they represent an easily accessible compartment both for immunomonitoring and for the prediction of vaccine efficacy.

Antigen-experienced memory CD8+ T cells constitute a diverse, heterogeneous cell population that is generated throughout life in response to viral infection (21, 22). In this study, we used genomic and immunological assays and characterized the phenotype, function, and immune gene signatures of human HSV-specific CD8+ T-cell subpopulations that share the same epitope specificity but were derived from either naturally protected ASYMP or nonprotected SYMP individuals. The present study confirmed our previous finding that a significant proportion of differentiated HSV-specific CD8+ T$_{EM}$ cells (CD45RA^{low} CCR7^{low} CD44^{high} CD62L^{low} CD8+) are maintained in the circulation of healthy ASYMP individuals. In contrast, higher frequencies of less differentiated CD8+ T$_{CM}$ cells (CD45RA^{low} CCR7^{high} CD44^{low} CD62L^{high} CD8+) are mostly present in SYMP patients. The ASYMP individuals had significantly higher proportions of multifunctional CD8+ T cells and simultaneously produced IFN-γ and expressed CD107$^{a/b}$, GzmB, GzmK, and perforin. In contrast, CD8+ T cells from SYMP individuals, which share the same epitope specificity, were mostly monofunctional. In addition, in this study we extended our previous finding by showing that human HSV-specific CD8+ T$_{EM}$ cells from ASYMP individuals expressed unique immune gene signatures that are consistent with an active JAK/STAT signaling pathway and expansion/survival cytokines. These unique gene signatures suggest that JAK/STAT, expansion, and expansion/survival features might be among key properties of protective HSV-specific CD8+ T cells. Thus, this does not rule out that other host or viral factors either alone or in concert with CD8+ T-cell responses also play an important role in determining the course of herpesvirus infection and disease. The ultimate underlying molecular mechanism by which CD8+ T cells contribute to the maintenance of the asymptomatic state was not defined by the present study. However, as illustrated in Fig. 8, the findings are consistent with a potential role of polyfunctional CD8+ T$_{EM}$ cells with unique gene signatures consistent with an active JAK/STAT pathway, type I IFN, and cytokines involved in T-cell survival and expansion (e.g., *JAK2*, *STAT3*, *STAT5B*, *IL-2*, *IL-4*, *IL-6*, *IL-6ST*, *IL-6R*, and *IL-7*) as protective in ASYMP individuals. We should emphasize that type I interferon, expansion/survival cytokines, and JAK/STAT pathways were affected only for HSV epitope-specific CD8+ T$_{EM}$ and T$_{CM}$ cells and not for bulk CD8+ T cells, suggesting that the effects occur only for CD8+ T cells that are specific to HSV-1, rather than being general systemic effects on all T cells. Unlike for CD8+ T cells, no significant difference in the phenotype and the function of CD4+ T cells was found between symptomatic and asymptomatic individuals. Hence, the present study focused on type I interferon, expansion/survival cytokines, and JAK/STAT gene signatures expressed by HSV-specific CD8+ T cells from symptomatic and asymptomatic individuals. A strict demonstration that CD8+ T cells from ASYMP individuals with these
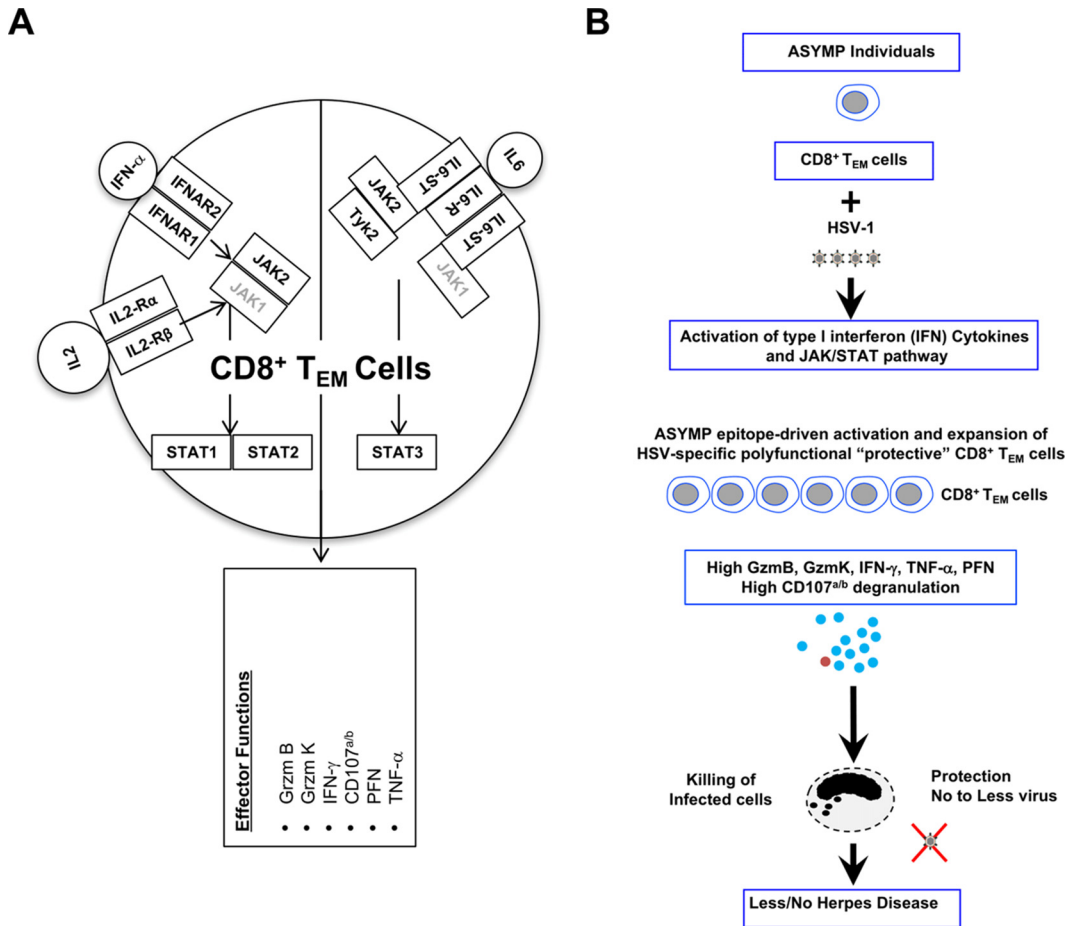
FIG 8 A proposed model of intracellular pathways engaged within, and functions of, HSV-specific CD8+ T cells from protected ASYMP individuals. (A) In ASYMP individuals, HSV-specific memory CD8+T cells develop more toward "protective" CD44high CD62Llow CD8+ T_{EM} cells. Cell surface receptors on CD8+ T_{EM} cells are engaged by IFN-γ, IL-6, and IL-2, leading to cell stimulation through JAK/STAT pathways. Activation of JAK1 and JAK3 mediates recruitment of STAT1, STAT2, and STAT3. (B) HSV-specific CD8+ T_{EM} cells from ASYMP individuals activated through type I interferon (IFN) and the JAK/STAT pathway proliferate and produce high levels of GzmB, GzmK, IFN-γ, tumor necrosis factor alpha (TNF-α), PFN, and CD107a/b, resulting in multifunctional CD8+ T cells that efficiently kill HSV-1-infected cells. Reduction in virus load leads to a decrease in recurrent herpetic disease.

genomic, phenotypic, and functional characteristic ensure immunologic control of recurrent corneal herpetic disease would require adoptive T-cell transfer experiments in SYMP humans or SYMP mice (2). Moreover, since the present study used a limited number (10 SYMP and 10 ASYMP) individuals, a much larger scale human study using T-cell samples from a larger number of SYMP and ASYMP individuals is needed to confirm that the unique type I interferon, expansion/survival cytokines, and JAK/STAT gene signatures of multifunctional HSV-specific effector memory CD8+ T_{EM} cells are associated with asymptomatic ocular herpes in humans.

Gene expression profiling studies reported herein used NanoString nCounter technologies to provide new insights into the nature of protective and nonprotective (or even pathogenic) CD8+ T cells in herpes infection (23, 24). These studies were able to compare the gene signatures of memory CD8+ T cells that shared the same HSV-1 antigenic specificity but were derived from either naturally protected ASYMP individuals or nonprotected SYMP individuals with a history of numerous episodes of recurrent herpetic disease. However, NanoString-based studies analyze the bulk CD8+ T-cell populations and therefore might not be able to evaluate heterogeneity among individual CD8+ T cells. Although we used epitope-specific CD8+ T cells sorted using single tetramers, the gene expression profile had been based on analyses of bulk CD8+ T-cell

populations and therefore may not be able to evaluate the heterogeneity among epitope-specific individual CD8+ T cells. This represents an important limitation because it is now appreciated that CD8+ T cells within the effector and memory populations exhibit substantial functional heterogeneity. This also makes it impossible to ascertain whether a divergence of HSV-specific memory CD8+ T-cell subsets has occurred in ASYMP compared to SYMP individuals. Moreover, the NanoString can target only up to 800 genes in a single reaction. These limitations underscore our current effort to develop single-cell transcriptomic approaches (i.e., whole-transcriptome shotgun sequencing [RNA-Seq]) to address fundamental questions such as the following. (i) Is there heterogeneity within the T_{CM} and T_{EM} cell subsets in SYMP and ASYMP individuals? (ii) Do memory CD8+ T-cell fates (T_{CM} and T_{EM}) diverge in ASYMP versus SYMP individuals? (iii) What are the molecular determinants that control the differentiation of memory CD8+ T cells into each of these memory subsets in SYMP and ASYMP individuals? Developing single-cell transcriptomic approaches, such as RNA-Seq, will help identify novel determinants of memory CD8+ T cells in SYMP versus ASYMP individuals and to interrogate molecular heterogeneity within memory CD8+ T-cell subsets at the single-cell level.

The present report supports our recently proposed "asymptomatic" immunotherapeutic vaccine strategy in which herpetic lesions can be treated by an asymptomatic T-cell-based immunotherapeutic vaccine that would induce an asymptomatic HSV-specific memory CD8+ T cells with genomic, phenotypic, and functional features, as illustrated in Fig. 8. Because of the obvious ethical and practical considerations of obtaining cornea-resident CD8+ T cells from statistically sufficient numbers of SYMP and ASYMP individuals, our investigations in SYMP versus ASYMP individuals were limited to blood-derived CD8+ T cells. We are aware that information gained from PBMC-derived T cells may not be completely reflective of tissue-resident CD8+ T cells (CD8+ T_{RM} cells). Nevertheless, the results for human cells presented here and previously reported mouse results (25–30) converge to suggest that ASYMP individuals mount faster and stronger polyfunctional HSV-specific CD8+ T_{EM} and CD8+ T_{RM} cell responses that allow for a better control of herpes reactivation and cure of recurrent disease. Moreover, this study used blood-derived CD8+ cells that are easily accessible for immunomonitoring and, hence, could help predict disease and vaccine efficacy.

JAK/STAT proteins and their negative regulators, the suppressors of cytokine signaling (SOCS) protein family, play central roles in regulating most cytokines important for T-cell responses (31–33). HSV-specific CD8+ T cells derived from ASYMP individuals appeared to express high levels of JAK2, STAT3, and STAT5. In contrast, HSV-specific CD8+ T cells derived from SYMP individuals expressed high levels of SOCS1 and SOCS3 but low levels of JAK2, STAT3, and STAT5. There are seven mammalian STAT family members: STAT1, STAT2, STAT3, STAT4, STAT5A, STAT5B, and STAT6. Most STAT proteins are primarily activated by membrane receptor-associated JAKs (31–33). Inhibition of the JAK/STAT signaling pathway by a JAK inhibitor abolished interferon (IFN)-mediated anti-HSV activity (27). Gene targeting studies have underscored the important role that SOCS1 and SOCS3 play in antagonizing responses to IFNs-STAT1 (34). Thus, downregulation of the JAK/STAT signaling pathway by SOCS1 and SOCS3 might interfere with IFN signaling, an efficient arm of herpes protective immunity (35). Interferons inhibit HSV replication in human cervical epithelial cells by activating the JAK/STAT pathway (27). Mott et al. have previously reported that HSV-1 replicated and produced viral mRNAs and DNA in dendritic cells (DCs) and macrophages from STAT1$^{-/-}$ deficient mice in contrast to DCs and macrophages from wild-type mice. These results suggest that the JAK-STAT pathway is involved in blocking replication of HSV-1 in DCs and macrophages (36). While activation of the JAK/STAT pathway appeared to be associated with protection against herpesvirus infection and disease, the mechanism by which JAK/STAT proteins are involved in herpes immunity remains to be fully elucidated and will be the subject of future reports.

In the present study, we found that CD8+ T cells from SYMP individuals have an increase in *SOCS1* and *SOCS3* genes, consistent with a mechanism of dysfunction in

cytokine expression. We also found that HSV-specific CD8$^+$ T cells from ASYMP individuals expressed higher levels of type I interferons (IFN-Is). The IFN-Is appear to be key drivers of inflammation and immunosuppression in chronic viral infection (37–40). Most cytokines use the JAK/STAT pathway, and this pathway is negatively regulated by suppressors of cytokine signaling (SOCS1 and SOCS3) proteins (31–33). Conversely, the *SOCS1* and *SOCS3* gene expression signature was significantly lower in CD8$^+$ T cells from ASYMP patients. The differential production of cytokine gene products was subsequently confirmed at the protein level using Luminex, and the levels of cytokine receptor genes were compared by FACS in HSV-specific CD8$^+$ T cells from SYMP and ASYMP individuals. These results suggest dysregulation of many T-cell expansion and survival cytokines/cytokine receptors in SYMP individuals by highly expressed SOCS proteins. This might have led to the reduction in CD8$^+$ T-cell immunity and hence exacerbation of herpetic diseases seen in SYMP individuals.

In this study, the expression of SOCS1 and SOCS3 proteins, two key regulators of inflammatory cytokines, was significantly increased in SYMP memory CD8$^+$ T cells compared to ASYMP memory CD8$^+$ T cells. SOCS proteins bind to many inflammatory cytokine receptors, thereby suppressing further inflammatory cytokine-mediated signaling events. Inflammatory cytokines shape CD8$^+$ T-cell responses (38–41). Previous studies have demonstrated that inflammatory cytokines dynamically fine-tune antigen sensitivity of antiviral CD8$^+$ T cells to help eliminate infected cells (41–43). Inflammation and CD8$^+$ T-cell interplay are reported in many pathological conditions of infections. Since many, if not most, cytokines important for T-cell responses utilize the JAK/STAT signaling pathway, which is negatively regulated by SOCS proteins, upregulation of SOCS signaling is expected to contribute to disruption of CD8$^+$ T-cell immunity in SYMP individuals. The mechanisms that lead to increased expression levels of SOCS genes in T cells from SYMP individuals remain to be determined. A direct role of the virus in T-cell dysfunction is not ruled out, as recent reports showed that HSV-1 infection of the T-cell lines rapidly induced SOCS3 (44). The induction of SOCS3 by HSV-1 occurs via STAT3 activation immediately after infection (31–33). SOCS3 induction was inhibited by the addition of a Jak3 inhibitor, WHI-P131, or by transfection of antisense oligonucleotides specific for SOCS3, which then dramatically suppressed replication of HSV-1 in T cells (44). Induction of SOCS3 appeared to be specific to T cells because monocytic cell lines U937 and THP-1 and the B-cell line AKATA showed no SOCS3 induction following HSV-1 infection (44). SOCS3 protein appears to be mainly responsible for the suppression of IFN signaling and IFN production that occurs during HSV-1 infection (45).

Over 50% of the world population is currently infected with HSV-1 (19, 27, 46). The majority of infected individuals remain asymptomatic (1, 3, 6, 7, 47–49), as they may have developed a "natural" protective immunity that protects from virus reactivation, symptomatic shedding, and/or recurrent herpes disease (49–51). In contrast, a much smaller population of SYMP individuals may have lost such immunity, causing them to develop frequent, recurrent herpetic disease (26, 30, 52). Although standard antiviral drugs can reduce recurrent symptomatic disease to some extent, they do not clear the infection (2, 53–56), making the development of a herpes vaccine an important priority. The results presented in this report shed some light on the genomic, phenotypic, and functional characterization of HSV-specific CD8$^+$ T-cell subpopulations from infected and naturally protected ASYMP individuals and could inform the development of an effective T-cell-based herpes therapeutic vaccine.

In summary, the present report provides several new insights about the phenotype, function, and gene signatures of blood-derived HSV-specific memory CD8$^+$ T cells that segregate with immunologic control of ocular herpes in ASYMP individuals. It confirms that CD8$^+$ T$_{EM}$ cells are associated with the control of ocular herpetic disease. Human HSV-1 epitopes predominately recalled polyfunctional CD8$^+$ T$_{EM}$ cells in ASYMP individuals. In contrast, the same HSV-1 epitopes tended to recall predominately monofunctional CD8$^+$ T$_{CM}$ cells in SYMP patients. Moreover, the study unraveled the JAK/STAT pathway and unique type I IFN and expansion and survival cytokine gene signatures that were expressed by HSV-specific memory CD8$^+$ T$_{EM}$ cells from naturally

protected ASYMP individuals. These gene signatures suggest an active JAK/STAT pathway and expansion/survival of antiviral CD8+ T_{EM} cells as key properties associated with protection. These quantitative and qualitative features of effective HSV-specific memory CD8+ T-cell responses should be taken into consideration in designing a T-cell-based herpes immunotherapeutic vaccine.

MATERIALS AND METHODS

Human study population. All clinical investigations in this study were conducted according to the Declaration of Helsinki. All subjects were enrolled at the University of California, Irvine, under approved institutional review board-approved protocols (IRB#2003-3111 and IRB#2009-6963). Written informed consent was received from all participants prior to inclusion in the study.

During the last 15 years (i.e., January 2003 to September 2018), we have screened 925 individuals for HSV-1 and HSV-2 seropositivity. Five hundred eighty-seven were white, 338 were nonwhite (African, Asian, Hispanic, and other), 458 were female, and 467 were male. Among this sample, a cohort of 726 immunocompetent individuals, ranging from 21 to 67 years old (median, 39), were seropositive for HSV-1 and seronegative for HSV-2. All patients were negative for HIV and hepatitis B virus (HBV), with no history of immunodeficiency. Seven hundred ninety-two patients were HSV-1, HSV-2, or HSV-1/HSV-2 seropositive, among whom 698 were healthy and defined as asymptomatic (ASYMP). These patients never had any herpes disease (ocular, genital, or dermal) based on self-reporting and clinical examination. Even a single episode of any herpetic disease would exclude the individual from this group. The remaining 94 patients were defined as HSV-seropositive symptomatic (SYMP) individuals who suffered from frequent and severe recurrent genital, ocular, and/or orofacial lesions. Signs of recurrent disease in SYMP patients were defined as herpetic lid lesions, herpetic conjunctivitis, dendritic or geographic keratitis, stromal keratitis, and iritis consistent with HSK, with one or more episodes per year for the past 2 years. However, at the time of blood collection, SYMP patients had no recurrent disease (other than corneal scarring) and had had no recurrences during the past 30 days. They had no ocular disease other than HSK, had no history of recurrent genital herpes, and were HSV-1 seropositive and HSV-2 seronegative. Because the spectrum of recurrent ocular herpetic disease is wide, our emphasis was mainly on the number of recurrent episodes and not on the severity of the recurrent disease. No attempt was made to assign specific T-cell epitopes to the severity of recurrent lesions. Patients were also excluded if they (i) had an active ocular (or elsewhere) herpetic lesion or had had one within the past 30 days, (ii) were seropositive for HSV-2, (iii) were pregnant or breastfeeding, or (iv) were on acyclovir and other related antiviral drugs or any other immunosuppressive drugs at the time of blood draw. Among this large cohort of SYMP and ASYMP individuals, 50 patients were enrolled in the current study (Table 1). SYMP and ASYMP groups were matched for age, gender, serological status, and race. We also collected and tested blood samples from 10 healthy control individuals who were seronegative for both HSV-1 and HSV-2 and had no history of ocular herpes, genital lesions, or orofacial herpes disease.

HSV-specific serotyping. The sera collected from random donors were tested for anti-HSV antibodies. Enzyme-linked immunosorbent assay (ELISA) was performed using sterile 96-well flat-bottom microplates coated with the HSV-1 antigen in coating buffer overnight at 4°C. The next day, plates were washed with phosphate-buffered saline (PBS)–1% Tween 20 (PBST) five times, and nonspecific binding was blocked by incubation with a 5% solution of skimmed milk in PBS (200 μl/well) at 4°C for 1 h at room temperature (RT). The microplates were washed three times with PBS-Tween and incubated with various sera at 37°C for 2 h. Following five washes, biotinylated rabbit anti-human IgG, diluted 1:20,000 with PBST, was incubated at 37°C for 2 h. After five washes, streptavidin was added at a 1:5,000 dilution and incubated for 30 min at RT. After five additional washes, the color was developed by adding 100 μl of 3,3′,5,5′-tetramethylbenzidine (TMB) substrate. The mixture was incubated for 5 to 15 min at RT in the absence of light. The reaction was terminated by adding 1 M H_2SO_4. The absorbance was measured at 450 nm.

HLA-A2 typing. The HLA-A2 status was confirmed by PBMC staining with 2 μl of anti-HLA-A2 MAb (clone BB7.2; BD Pharmingen, Franklin Lakes, NJ) at 4°C for 30 min. The cells were washed and analyzed by flow cytometry using an LSRII (Becton, Dickinson, Franklin Lakes, NJ). The acquired data were analyzed with FlowJo software (BD Biosciences, San Jose, CA).

Peripheral blood mononuclear cell isolation. Individuals (negative for HIV and HBV and with or without any HSV infection history) were recruited at the UC Irvine Institute for Clinical and Translational Science (ICTS). One hundred milliliters of blood was drawn into yellow-top Vacutainer tubes (Becton, Dickinson). The serum was isolated and stored at −80°C for the detection of anti-HSV-1 and anti-HSV-2 antibodies, as we have previously described (9). Peripheral blood mononuclear cells (PBMCs) were isolated by gradient centrifugation using leukocyte separation medium (Life Sciences, Tewksbury, MA). The cells were then washed in PBS and resuspended in complete culture medium consisting of RPMI 1640 and 10% fetal bovine serum (FBS) (Bio-Products, Woodland, CA) supplemented with 1× penicillin–streptomycin–L-glutamine, 1× sodium pyruvate, 1× nonessential amino acids, and 50 μM 2-mercaptoethanol (Life Technologies, Rockville, MD).

Peptide synthesis. HLA-A*0201 binding peptides (9-mer long) corresponding to immunodominant human CD8+ T-cell epitopes from four HSV-1 proteins—$gB_{561-567}$ (RMLGDVMAV), $VP11/12_{220-228}$ (RLNE LLAYV), $UL43_{302-310}$ (FLGGHVAVA), and $UL44_{400-408}$ (FLGGDDPSPA)—were synthesized using solid-phase peptide synthesis and standard 9-fluorenylmethoxy carbonyl technology (PE Applied Biosystems, Foster City, CA). The purity of peptides was over 90%, as determined by reversed-phase high-performance liquid chromatography (Vydac C_{18}) and mass spectroscopy (Voyager MALDI-TOF system). Stock solutions were

made at 1 mg/ml in 10% dimethyl sulfoxide (DMSO) in PBS. All peptides were aliquoted and stored at −20°C until assayed.

Flow cytometry assays. Peripheral blood mononuclear cells were analyzed by flow cytometry after staining with fluorochrome-conjugated human-specific MAbs. The following anti-human antibodies were used for the flow cytometry assays: CD3 (clone SK7) phycoerythrin (PE)-Cy7, CD44 (clone G44-26) A700, CD8 (clone SK1) allophycocyanin (APC)-Cy7, CCR7 (clone 150503) Alexa Fluor 700, CD45RA fluorescein isothiocyanate (FITC), CD62L allophycocyanin, IFNAR2 (clone REA124) APC, IL-6R (clone UV4) APC, IL-7R (clone A019D5) FITC, IL-2R gamma (clone 633162) Alexa Fluor 700, IFN-γ Alexa Fluor 647, granzyme B (clone GB11) A647, CD107a (clone H4A3) FITC, CD107b (clone H4B4) FITC (BioLegend), granzyme K (clone G3H69) peridinin chlorophyll protein-eFluor 710, and perforin (clone d69) FITC. Surface-staining MAbs against various cell markers were added to a total of 1×10^6 PBMCs in PBS containing 1% FBS and 0.1% sodium azide (FACS buffer) for 45 min at 4°C. After the cells were washed with FACS buffer, they were permeabilized for 20 min on ice using a Cytofix/Cytoperm kit (BD Biosciences) and then washed twice with Perm/Wash buffer (BD Bioscience). Intracellular cytokine-staining MAbs were added to the cells, and the mixture was incubated for 45 min on ice in the dark. The cells were washed with Perm/Wash buffer and FACS buffer and subsequently fixed in PBS containing 2% paraformaldehyde (Sigma-Aldrich, St. Louis, MO). For each sample, 100,000 total events were acquired on the BD LSRII. Ab capture beads (BD Biosciences) were used as individual compensation tubes for each fluorophore in the experiment. To define positive and negative populations, we employed fluorescence minus controls for each fluorophore used in this study when initially developing staining protocols. In addition, we further optimized gating by examining known negative cell populations for background expression levels. The gating strategy was similar to that used in our previous work (3). Briefly, we gated single cells, viable cells (aqua blue), lymphocytes, CD3+ cells, and CD8+ cells before finally gating human epitope-specific CD8+ T cells using HSV-specific tetramers. Data analysis was performed using FlowJo version 10.4.2 (TreeStar, Ashland, OR). Statistical analyses were done using GraphPad Prism version 5 (La Jolla, CA).

NanoString analysis. The NanoString assay includes three main steps: hybridization, purification and immobilization; counting; and analysis. For hybridization, a population of RNA is mixed with the probes in the solution. Each target molecule, without the need for amplification, is then hybridized directly to the unique color-coded barcodes. For purification and immobilization, after hybridization, excess probes are removed by washing and the probe-target complexes are bound, immobilized, and aligned on the nCounter cartridge. Each color-coded barcode represents a single target molecule. The expression level of the target gene is measured by counting the number of times that the unique color-coded barcode of the target gene is detected. The barcode counts are measured directly and then tabulated. Each color-coded barcode represents a single target molecule.

Raw data were normalized based on the geometric mean of negative controls, internal housekeeping genes, and positive controls in nSolver 3.0. Normalized counts from genes included in immune panels and fulfilling the minimum count requirement were averaged before additional analysis.

We used a commercially available human gene panel, nCounter Immunology v2 (human), containing 579 unique human genes (Table 2) known to be broadly relevant in the immune responses, including 15 housekeeping genes and six positive controls (NanoString Technologies, Seattle, WA). HSV-specific CD8+ T cells were FACS sorted from either SYMP, ASYMP, or seronegative individuals using human tetramers specific to immunodominant epitopes selected from both glycoproteins and tegument proteins: (i) an envelope protein (UL43$_{302-310}$), (ii) glycoprotein C (UL44$_{400-408}$), (iii) glycoprotein B (gB$_{561-567}$), and (iv) the tegument protein VP11/12 (VP11/12$_{220-228}$). RNA was isolated from the sorted cells using the Direct-zol RNS MiniPrep (Zymo Research, Irvine, CA) according to the manufacturer's instructions. RNA concentrations were determined by NanoDrop (Thermo Scientific, Wimington, DE). Reporter and capture probes were hybridized during a 20-h incubation at 65°C, and the resulting RNA complexes were subsequently immobilized and counted on an nCounter analyzer (NanoString Technologies, Seattle, WA) according to the manufacturer's instructions.

Raw data were normalized based on the geometric mean of negative controls, internal housekeeping genes, and positive controls in nSolver 3.0. Normalized counts from genes included in immune panels and fulfilling the minimum count requirement were averaged before additional analysis.

Luminex assay. A total of 10×10^6 PBMCs from either SYMP or ASYMP were cultured in RPMI 1640 supplemented with 10% FBS (Bio-Products, Woodland, CA) and 1× penicillin-streptomycin. The cells were stimulated with four different peptides individually, i.e., gB$_{561-567}$, VP11/12$_{220-228}$, UL43$_{302-310}$, or UL44$_{400-408}$, at a concentration of 10 μg/ml. On day 2, the supernatant was collected. The concentrations of the cytokines were determined using the Luminex MAGPIX analyzer (Luminex; XMAP Technology), and data were analyzed and expressed as median fluorescence intensity (MFI) and concentration (picograms per milliliter).

Production of IFN-γ and expression of CD107a/b, GzmB, GzmK, and PFN cytotoxic markers. To detect cytolytic CD8+ T cells recognizing peptides in freshly isolated PBMCs, we performed an intracellular IFN-γ and CD107a/b cytotoxicity assay. Betts and colleagues have described the CD107a/b assay as an alternative cytotoxicity assay that can address some of the shortcomings of the 51Cr release assay. The intracellular assay to detect IFN-γ and CD107a/b, GzmB, GzmK, and PFN cytotoxic markers in response to in vitro peptide stimulations was performed as described with a few modifications (38, 40, 57). On the day of the assay, 1×10^6 PBMCs were stimulated in vitro with individual peptide (1 μg/ml of peptide) at 37°C for additional 6 h in a 96-well plate with BD Golgi Stop (BD Biosciences) and 10 μl of CD107a FITC and CD107b FITC. Phytohemagglutinin (PHA; 5 μg/ml; Sigma) and no peptide were used as positive and negative controls, respectively. At the end of the incubation period, the cells were transferred to a 96-well round-bottom plate, washed twice with FACS buffer, and then stained with PE-conjugated anti-human

CD8 for 45 min at 4°C. The intracellular staining for the detection of IFN-γ and CD107$^{a/b}$ was performed as outlined above. The cells were rewashed and fixed, and 500,000 total events were acquired on the BD LSRII. Data analysis was performed using FlowJo version 9.9.4 (TreeStar, Ashland, OR).

T-cell proliferation assay (Ki-67). CD8⁺ T-cell proliferation was measured using a Ki67 mAb as recently described (2, 47). Briefly, PBMCs were first stained with PE-conjugated mAb specific to human CD8⁺ molecules. In 1× PBS at room temperature. Cold FCS was then added, and cells were washed extensively with RPMI 1640 plus 10% FCS. Afterward, the cells were stained intracellularly with Ki-67 antibody. In the later part of the experiment, cells were rewashed and fixed, and 500,000 total events were acquired on the BD LSRII. Data analysis was performed using FlowJo version 9.9.4 (TreeStar, Ashland, OR).

Statistical analysis. We examined the distribution of each immunological parameter. In the case of two group comparisons, we used the parametric two-sample t test or nonparametric Wilcoxon rank sum test, as appropriate. For parameters satisfying a normal distribution, we used the F-test for equality of variances to determine if it would be appropriate to apply the Satterthwaite test assuming unequal variances between groups. The nominal P values in the corresponding figures after correction for multiple comparisons are reported. In the specific case of three groups (i.e., comparing SYMP and ASYMP subgroups with a baseline seronegative [NEG] subgroup), we used the general linear model procedure and compared the least-squares means using the Dunnett procedure for multiple comparisons. Flow cytometry data were analyzed with FlowJo software (TreeStar). For analysis, we used SAS v.9.4 (Statistical Analysis System, Cary, NC). Graphs were prepared with GraphPad Prism software (San Diego, CA). Data are expressed as means + standard deviations (SD). Error bars show standard errors of the means (SEM).

REFERENCES

1. Zhang X, Dervillez X, Chentoufi AA, Badakhshan T, Bettahi I, Benmohamed L. 2012. Targeting the genital tract mucosa with a lipopeptide/recombinant adenovirus prime/boost vaccine induces potent and long-lasting CD8+ T cell immunity against herpes: importance of MyD88. J Immunol 189:4496–4509. https://doi.org/10.4049/jimmunol.1201121.
2. Chentoufi AA, Dasgupta G, Christensen ND, Hu J, Choudhury ZS, Azeem A, Jester JV, Nesburn AB, Wechsler SL, BenMohamed L. 2010. A novel HLA (HLA-A*0201) transgenic rabbit model for preclinical evaluation of human CD8+ T cell epitope-based vaccines against ocular herpes. J Immunol 184:2561–2571. https://doi.org/10.4049/jimmunol.0902322.
3. Chentoufi AA, Zhang X, Lamberth K, Dasgupta G, Bettahi I, Nguyen A, Wu M, Zhu X, Mohebbi A, Buus S, Wechsler SL, Nesburn AB, BenMohamed L. 2008. HLA-A*0201-restricted CD8+ cytotoxic T lymphocyte epitopes identified from herpes simplex virus glycoprotein D. J Immunol 180:426–437. https://doi.org/10.4049/jimmunol.180.1.426.
4. Chentoufi AA, BenMohamed L, Van De Perre P, Ashkar AA. 2012. Immunity to ocular and genital herpes simplex viruses infections. Clin Dev Immunol 2012:732546. https://doi.org/10.1155/2012/732546.
5. Chentoufi AA, Benmohamed L. 2012. Mucosal herpes immunity and immunopathology to ocular and genital herpes simplex virus infections. Clin Dev Immunol 2012:149135. https://doi.org/10.1155/2012/149135.
6. Corey L, Langenberg AG, Ashley R, Sekulovich RE, Izu AE, Douglas JM, Jr, Handsfield HH, Warren T, Marr L, Tyring S, DiCarlo R, Adimora AA, Leone P, Dekker CL, Burke RL, Leong WP, Straus SE. 1999. Recombinant glycoprotein vaccine for the prevention of genital HSV-2 infection: two randomized controlled trials. Chiron HSV Vaccine Study Group. JAMA 282:331–340.
7. Langenberg AG, Corey L, Ashley RL, Leong WP, Straus SE. 1999. A prospective study of new infections with herpes simplex virus type 1 and type 2. Chiron HSV Vaccine Study Group. N Engl J Med 341:1432–1438. https://doi.org/10.1056/NEJM199911043411904.
8. Dasgupta G, BenMohamed L. 2011. Of mice and not humans: how reliable are animal models for evaluation of herpes CD8(+)-T cell-epitopes-based immunotherapeutic vaccine candidates?. Vaccine 29:5824–5836. https://doi.org/10.1016/j.vaccine.2011.06.083.
9. Chentoufi AA, Binder NR, Berka N, Durand G, Nguyen A, Bettahi I, Maillere B, BenMohamed L. 2008. Asymptomatic human CD4+ cytotoxic T-cell epitopes identified from herpes simplex virus glycoprotein B. J Virol 82:11792–11802. https://doi.org/10.1128/JVI.00692-08.
10. BenMohamed L, Bertrand G, McNamara CD, Gras-Masse H, Hammer J, Wechsler SL, Nesburn AB. 2003. Identification of novel immunodominant CD4+ Th1-type T-cell peptide epitopes from herpes simplex virus glycoprotein D that confer protective immunity. J Virol 77:9463–9473. https://doi.org/10.1128/JVI.77.17.9463-9473.2003.
11. Zhang X, Issagholian A, Berg EA, Fishman JB, Nesburn AB, BenMohamed L. 2005. Th-cytotoxic T-lymphocyte chimeric epitopes extended by Nepsilon-palmitoyl lysines induce herpes simplex virus type 1-specific effector CD8+ Tc1 responses and protect against ocular infection. J Virol 79:15289–15301. https://doi.org/10.1128/JVI.79.24.15289-15301.2005.
12. Nesburn AB, Bettahi I, Zhang X, Zhu X, Chamberlain W, Afifi RE, Wechsler SL, BenMohamed L. 2006. Topical/mucosal delivery of sub-unit vaccines that stimulate the ocular mucosal immune system. Ocul Surf 4:178–187. https://doi.org/10.1016/S1542-0124(12)70164-7.
13. Agelidis AM, Shukla D. 2015. Cell entry mechanisms of HSV: what we have learned in recent years. Future Virol 10:1145–1154. https://doi.org/10.2217/fvl.15.85.
14. Joshi NS, Cui W, Dominguez CX, Chen JH, Hand TW, Kaech SM. 2011. Increased numbers of preexisting memory CD8 T cells and decreased T-bet expression can restrain terminal differentiation of secondary effector and memory CD8 T cells. J Immunol 187:4068–4076. https://doi.org/10.4049/jimmunol.1002145.
15. Jung YW, Rutishauser RL, Joshi NS, Haberman AM, Kaech SM. 2010.

Differential localization of effector and memory CD8 T cell subsets in lymphoid organs during acute viral infection. J Immunol 185:5315–5325. https://doi.org/10.4049/jimmunol.1001948.

16. Joshi NS, Kaech SM. 2008. Effector CD8 T cell development: a balancing act between memory cell potential and terminal differentiation. J Immunol 180:1309–1315. https://doi.org/10.4049/jimmunol.180.3.1309.

17. Chandele A, Joshi NS, Zhu J, Paul WE, Leonard WJ, Kaech SM. 2008. Formation of IL-7Ralphahigh and IL-7Ralphalow CD8 T cells during infection is regulated by the opposing functions of GABPalpha and Gfi-1. J Immunol 180:5309–5319. https://doi.org/10.4049/jimmunol.180.8.5309.

18. Joshi NS, Cui W, Chandele A, Lee HK, Urso DR, Hagman J, Gapin L, Kaech SM. 2007. Inflammation directs memory precursor and short-lived effector CD8(+) T cell fates via the graded expression of T-bet transcription factor. Immunity 27:281–295. https://doi.org/10.1016/j.immuni.2007.07.010.

19. Samandary S, Kridane-Miledi H, Sandoval JS, Choudhury Z, Langa-Vives F, Spencer D, Chentoufi AA, Lemonnier FA, BenMohamed L. 2014. Associations of HLA-A, HLA-B and HLA-C alleles frequency with prevalence of herpes simplex virus infections and diseases across global populations: implication for the development of an universal CD8+ T-cell epitope-based vaccine. Hum Immunol 75:715–729. https://doi.org/10.1016/j.humimm.2014.04.016.

20. Dervillez X, Qureshi H, Chentoufi AA, Khan AA, Kritzer E, Yu DC, Diaz OR, Gottimukkala C, Kalantari M, Villacres MC, Scarfone VM, McKinney DM, Sidney J, Sette A, Nesburn AB, Wechsler SL, BenMohamed L. 2013. Asymptomatic HLA-A*02:01-restricted epitopes from herpes simplex virus glycoprotein B preferentially recall polyfunctional CD8+ T cells from seropositive asymptomatic individuals and protect HLA transgenic mice against ocular herpes. J Immunol 191:5124–5138. https://doi.org/10.4049/jimmunol.1301415.

21. Snell LM, MacLeod BL, Law JC, Osokine I, Elsaesser HJ, Hezaveh K, Dickson RJ, Gavin MA, Guidos CJ, McGaha TL, Brooks DG. 2018. CD8(+) T cell priming in established chronic viral infection preferentially directs differentiation of memory-like cells for sustained immunity. Immunity 49:678–694.e5. https://doi.org/10.1016/j.immuni.2018.08.002.

22. Snell LM, Osokine I, Yamada DH, De la Fuente JR, Elsaesser HJ, Brooks DG. 2016. Overcoming CD4 Th1 cell fate restrictions to sustain antiviral CD8 T cells and control persistent virus infection. Cell Rep 16:3286–3296. https://doi.org/10.1016/j.celrep.2016.08.065.

23. Szeles L, Meissner F, Dunand-Sauthier I, Thelemann C, Hersch M, Singovski S, Haller S, Gobet F, Fuertes Marraco SA, Mann M, Garcin D, Acha-Orbea H, Reith W. 2015. TLR3-mediated CD8+ dendritic cell activation is coupled with establishment of a cell-intrinsic antiviral state. J Immunol 195:1025–1033. https://doi.org/10.4049/jimmunol.1402033.

24. Chang JJ, Woods M, Lindsay RJ, Doyle EH, Griesbeck M, Chan ES, Robbins GK, Bosch RJ, Altfeld M. 2013. Higher expression of several interferon-stimulated genes in HIV-1-infected females after adjusting for the level of viral replication. J Infect Dis 208:830–838. https://doi.org/10.1093/infdis/jit262.

25. Jiang X, Brown D, Osorio N, Hsiang C, BenMohamed L, Wechsler SL. 2016. Increased neurovirulence and reactivation of the herpes simplex virus type 1 latency-associated transcript (LAT)-negative mutant dLAT2903 with a disrupted LAT miR-H2. J Neurovirol 22:38–49. https://doi.org/10.1007/s13365-015-0362-y.

26. BenMohamed L, Osorio N, Khan AA, Srivastava R, Huang L, Krochmal JJ, Garcia JM, Simpson JL, Wechsler SL. 2016. Prior corneal scarification and injection of immune serum are not required before ocular HSV-1 infection for UV-B-induced virus reactivation and recurrent herpetic corneal disease in latently infected mice. Curr Eye Res 41:747–756. https://doi.org/10.3109/02713683.2015.1061024.

27. Srivastava R, Khan AA, Garg S, Syed SA, Furness JN, Vahed H, Pham T, Yu HT, Nesburn AB, BenMohamed L. 2017. Human asymptomatic epitopes identified from the herpes simplex virus tegument protein VP13/14 (UL47) preferentially recall polyfunctional effector memory CD44high CD62Llow CD8+ TEM cells and protect humanized HLA-A*02:01 transgenic mice against ocular herpesvirus infection. J Virol 91:e01793-16. https://doi.org/10.1128/JVI.01793-16.

28. Khan AA, Srivastava R, Chentoufi AA, Kritzer E, Chilukuri S, Garg S, Yu DC, Vahed H, Huang L, Syed SA, Furness JN, Tran TT, Anthony NB, McLaren CE, Sidney J, Sette A, Noelle RJ, BenMohamed L. 2017. Bolstering the number and function of HSV-1-specific CD8+ effector memory T cells and tissue-resident memory T cells in latently infected trigeminal gan-

29. Srivastava R, Dervillez X, Khan AA, Chentoufi AA, Chilukuri S, Shukr N, Fazli Y, Ong NN, Afifi RE, Osorio N, Geertsema R, Nesburn AB, Wechsler SL, BenMohamed L. 2016. The herpes simplex virus latency-associated transcript gene is associated with a broader repertoire of virus-specific exhausted CD8+ T cells retained within the trigeminal ganglia of latently infected HLA transgenic rabbits. J Virol 90:3913–3928. https://doi.org/10.1128/JVI.02450-15.

30. Srivastava R, Khan AA, Spencer D, Vahed H, Lopes PP, Thai NT, Wang C, Pham TT, Huang J, Scarfone VM, Nesburn AB, Wechsler SL, BenMohamed L. 2015. HLA-A02:01-restricted epitopes identified from the herpes simplex virus tegument protein VP11/12 preferentially recall polyfunctional effector memory CD8+ T cells from seropositive asymptomatic individuals and protect humanized HLA-A*02:01 transgenic mice against ocular herpes. J Immunol 194:2232–2248. https://doi.org/10.4049/jimmunol.1402606.

31. Crawley AM, Vranjkovic A, Faller E, McGuinty M, Busca A, Burke SC, Cousineau S, Kumar A, Macpherson PA, Angel JB. 2014. Jak/STAT and PI3K signaling pathways have both common and distinct roles in IL-7-mediated activities in human CD8+ T cells. J Leukoc Biol 95:117–127. https://doi.org/10.1189/jlb.0313122.

32. Verdeil G, Chaix J, Schmitt-Verhulst AM, Auphan-Anezin N. 2006. Temporal cross-talk between TCR and STAT signals for CD8 T cell effector differentiation. Eur J Immunol 36:3090–3100. https://doi.org/10.1002/eji.200636347.

33. Schade AE, Wlodarski MW, Maciejewski JP. 2006. Pathophysiology defined by altered signal transduction pathways: the role of JAK-STAT and PI3K signaling in leukemic large granular lymphocytes. Cell Cycle 5:2571–2574. https://doi.org/10.4161/cc.5.22.3449.

34. Schindler C, Levy DE, Decker T. 2007. JAK-STAT signaling: from interferons to cytokines. J Biol Chem 282:20059–20063. https://doi.org/10.1074/jbc.R700016200.

35. Li YL, Li HJ, Ji F, Zhang X, Wang R, Hao JQ, Bi WX, Dong L. 2010. Thymic stromal lymphopoietin promotes lung inflammation through activation of dendritic cells. J Asthma 47:117–123. https://doi.org/10.3109/02770900903483816.

36. Mott KR, Underhill D, Wechsler SL, Town T, Ghiasi H. 2009. A role for the JAK-STAT1 pathway in blocking replication of HSV-1 in dendritic cells and macrophages. Virol J 6:56. https://doi.org/10.1186/1743-422X-6-56.

37. Snell LM, McGaha TL, Brooks DG. 2017. Type I interferon in chronic virus infection and cancer. Trends Immunol 38:542–557. https://doi.org/10.1016/j.it.2017.05.005.

38. Sun J, Rajsbaum R, Yi M. 2015. Immune and non-immune responses to hepatitis C virus infection. World J Gastroenterol 21:10739–10748. https://doi.org/10.3748/wjg.v21.i38.10739.

39. Fruh K, Picker L. 2017. CD8+ T cell programming by cytomegalovirus vectors: applications in prophylactic and therapeutic vaccination. Curr Opin Immunol 47:52–56. https://doi.org/10.1016/j.coi.2017.06.010.

40. Hansen SG, Powers CJ, Richards R, Ventura AB, Ford JC, Siess D, Axthelm MK, Nelson JA, Jarvis MA, Picker LJ, Fruh K. 2010. Evasion of CD8+ T cells is critical for superinfection by cytomegalovirus. Science 328:102–106. https://doi.org/10.1126/science.1185350.

41. Wilson EB, Brooks DG. 2013. Inflammation makes T cells sensitive. Immunity 38:5–7. https://doi.org/10.1016/j.immuni.2013.01.001.

42. Richer MJ, Nolz JC, Harty JT. 2013. Pathogen-specific inflammatory milieux tune the antigen sensitivity of CD8(+) T cells by enhancing T cell receptor signaling. Immunity 38:140–152. https://doi.org/10.1016/j.immuni.2012.09.017.

43. Raue HP, Beadling C, Haun J, Slifka MK. 2013. Cytokine-mediated programmed proliferation of virus-specific CD8(+) memory T cells. Immunity 38:131–139. https://doi.org/10.1016/j.immuni.2012.09.019.

44. Yokota S, Yokosawa N, Okabayashi T, Suzutani T, Fujii N. 2005. Induction of suppressor of cytokine signaling-3 by herpes simplex virus type 1 confers efficient viral replication. Virology 338:173–181. https://doi.org/10.1016/j.virol.2005.04.028.

45. Yokota S, Yokosawa N, Okabayashi T, Suzutani T, Miura S, Jimbow K, Fujii N. 2004. Induction of suppressor of cytokine signaling-3 by herpes simplex virus type 1 contributes to inhibition of the interferon signaling pathway. J Virol 78:6282–6286. https://doi.org/10.1128/JVI.78.12.6282-6286.2004.

46. Looker KJ, Garnett GP, Schmid GP. 2008. An estimate of the global prevalence and incidence of herpes simplex virus type 2 infection.

Bull World Health Organ 86:805–812. https://doi.org/10.2471/BLT.07.046128.

47. Chentoufi AA, BenMohamed L. 2010. Future viral vectors for the delivery of asymptomatic herpes epitope-based immunotherapeutic vaccines. Future Virol 5:525–528. https://doi.org/10.2217/fvl.10.44.

48. Chentoufi AA, Dervillez X, Dasgupta G, Nguyen C, Kabbara KW, Jiang X, Nesburn AB, Wechsler SL, BenMohamed L. 2012. The herpes simplex virus type 1 latency-associated transcript inhibits phenotypic and functional maturation of dendritic cells. Viral Immunol 25:204–215. https://doi.org/10.1089/vim.2011.0091.

49. Khan AA, Srivastava R, Chentoufi AA, Geertsema R, Thai NT, Dasgupta G, Osorio N, Kalantari M, Nesburn AB, Wechsler SL, BenMohamed L. 2015. Therapeutic immunization with a mixture of herpes simplex virus 1 glycoprotein D-derived "asymptomatic" human CD8+ T-cell epitopes decreases spontaneous ocular shedding in latently infected HLA transgenic rabbits: association with low frequency of local PD-1+ TIM-3+ CD8+ exhausted T cells. J Virol 89:6619–6632. https://doi.org/10.1128/JVI.00788-15.

50. Dervillez X, Gottimukkala C, Kabbara KW, Nguyen C, Badakhshan T, Kim SM, Nesburn AB, Wechsler SL, Benmohamed L. 2012. Future of an "asymptomatic" T-cell epitope-based therapeutic herpes simplex vaccine. Future Virol 7:371–378. https://doi.org/10.2217/fvl.12.22.

51. Kuo T, Wang C, Badakhshan T, Chilukuri S, BenMohamed L. 2014. The challenges and opportunities for the development of a T-cell epitope-based herpes simplex vaccine. Vaccine 32:6733–6745. https://doi.org/10.1016/j.vaccine.2014.10.002.

52. BenMohamed L, Osorio N, Srivastava R, Khan AA, Simpson JL, Wechsler SL. 2015. Decreased reactivation of a herpes simplex virus type 1 (HSV-1) latency-associated transcript (LAT) mutant using the in vivo mouse UV-B model of induced reactivation. J Neurovirol 21:508–517. https://doi.org/10.1007/s13365-015-0348-9.

53. Chentoufi AA, Dasgupta G, Nesburn AB, Bettahi I, Binder NR, Choudhury ZS, Chamberlain WD, Wechsler SL, BenMohamed L. 2010. Nasolacrimal duct closure modulates ocular mucosal and systemic CD4(+) T-cell responses induced following topical ocular or intranasal immunization. Clin Vaccine Immunol 17:342–353. https://doi.org/10.1128/CVI.00347-09.

54. Dasgupta G, Nesburn AB, Wechsler SL, BenMohamed L. 2010. Developing an asymptomatic mucosal herpes vaccine: the present and the future. Future Microbiol 5:1–4. https://doi.org/10.2217/fmb.09.101.

55. Dasgupta G, Chentoufi AA, Nesburn AB, Wechsler SL, BenMohamed L. 2009. New concepts in herpes simplex virus vaccine development: notes from the battlefield. Expert Rev Vaccines 8:1023–1035. https://doi.org/10.1586/erv.09.60.

56. Zhang X, Chentoufi AA, Dasgupta G, Nesburn AB, Wu M, Zhu X, Carpenter D, Wechsler SL, You S, BenMohamed L. 2009. A genital tract peptide epitope vaccine targeting TLR-2 efficiently induces local and systemic CD8+ T cells and protects against herpes simplex virus type 2 challenge. Mucosal Immunol 2:129–143. https://doi.org/10.1038/mi.2008.81.

57. Betts MR, Brenchley JM, Price DA, De Rosa SC, Douek DC, Roederer M, Koup RA. 2003. Sensitive and viable identification of antigen-specific CD8+ T cells by a flow cytometric assay for degranulation. J. Immunol Methods 281(1-2):65–78. https://doi.org/10.1016/S0022-1759(03)00265-5.